# Accepted Manuscript


Spirohydantoins and 1,2,4-triazole-3-carboxamide derivatives as inhibitors of histone deacetylase: Design, synthesis, and biological evaluation

Alshimaa M.A. Aboeldahab, Eman A.M. Beshr, Mai E. Shoman, Safwat M. Rabea, Omar M. Aly

PII: S0223-5234(18)30021-7

DOI: 10.1016/j.ejmech.2018.01.021

Reference: EJMECH 10098

To appear in: *European Journal of Medicinal Chemistry*

Received Date: 25 August 2017

Revised Date: 22 December 2017

Accepted Date: 8 January 2018

Please cite this article as: A.M.A. Aboeldahab, E.A.M. Beshr, M.E. Shoman, S.M. Rabea, O.M. Aly, Spirohydantoins and 1,2,4-triazole-3-carboxamide derivatives as inhibitors of histone deacetylase: Design, synthesis, and biological evaluation, *European Journal of Medicinal Chemistry* (2018), doi: 10.1016/j.ejmech.2018.01.021.

## Graphical abstract

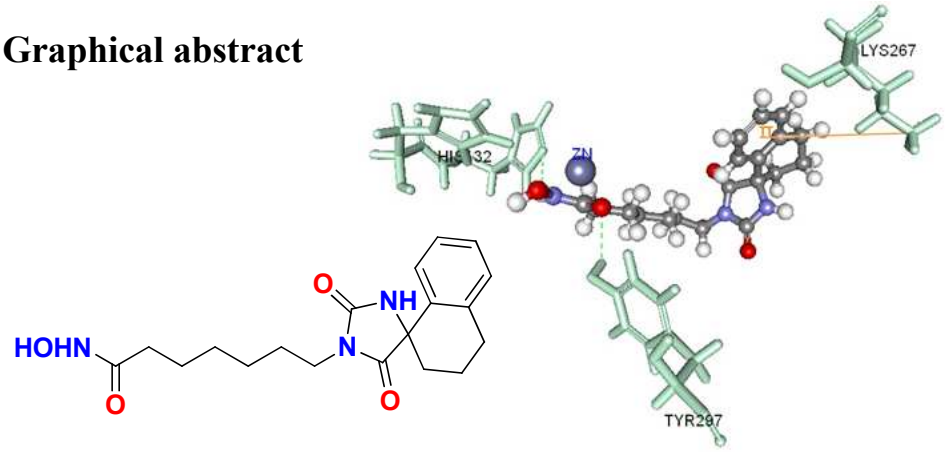


Compound **5f** (Docked into HDLP active site) showed comparable cytotoxicity and HDAC inhibitory activity to SAHA

# Spirohydantoins and 1,2,4-Triazole-3-Carboxamide Derivatives as Inhibitors of Histone Deacetylase: Design, Synthesis, and Biological Evaluation

Alshimaa M. A. Aboeldahab [a], Eman A. M. Beshr [a], Mai E. Shoman [a], Safwat M. Rabea [b], Omar M. Aly [a,c]*.

[a] Medicinal Chemistry Department, Faculty of Pharmacy, Minia University, Minia 61519, Egypt.

[b] Faculty of Pharmaceutical Sciences, The University of British Columbia, Vancouver, BC V6T 1Z3 Canada.

[C] College of Clinical Pharmacy, Albaha University, Kingdom of Saudi Arabia

*Corresponding author

E-mail addresses: omarsokkar@yahoo.com; omarsokkar@mu.edu.eg

*Abstract*

Two structurally novel series of histone deacetylase inhibitors (HDACIs) involving two potential surface recognition moieties; 3',4'-dihydro-2'*H*-spiro[imidazolidine-4,1'-naphthalene]-2,5-dione (in series I) and 1-(3-methoxyphenyl)-5-(3,4,5-trimethoxyphenyl)-1H-1,2,4-triazole-3-carboxamide (in series II) were designed, synthesized, and evaluated for their anti-proliferative activities, HDAC inhibitory activities, and their binding modes to HDAC protein. Compounds **5f** and **10e** showed comparable HDAC inhibitory activity to SAHA.

Series II have been also demonstrated as potential HDAC-tubulin dual inhibitors, promoted with structural similarities between (1-(3-methoxyphenyl)-5-(3,4,5-trimethoxyphenyl)-1H-1,2,4-triazole-3-carboxamide) nucleus, of series II, and Combretastatin A4.

The tubulin inhibitory activities of series II members, together with their docking into colchicine binding site of β-tubulin were performed. Compound **9a** showed remarkable cytotoxicity. Hybrid **10e** behaved as potent HDAC-tubulin dual inhibitor. It showed better tubulin inhibition than CA4 as well as its effectiveness against HDAC.

*Key words:* HDAC; Epigenetics; Spirohydantoin; Triazole.

## 1. *Introduction*

Cancer is mainly a disease of tissue growth regulation failure, which its initiation and progression is controlled by genetic (by mutation) and epigenetic (by deregulation) processes [1, 2]. Among the epigenetic events is acetylation/deacetylation of histone *N*-terminal lysine, which obviously leads to changes in gene expression through change of chromatin structure without changing gene sequence [3]. The turnover of the acetyl groups on histone tail occurs normally in the cells and the level of acetylation is controlled by the equilibrium between activities of two enzymes; histone acetyl transferases (HATs) and histone deacetylases (HDACs) [4]. HATs neutralize the positive charge of lysine residues in the *N*-terminal tail of histone, by adding an acetyl group, allowing the phosphate backbone of the DNA to open up and relax, thus, facilitates the accessibility of a variety of factors to DNA and the transcriptional activation of many genes including tumor suppressor genes silenced in cancer [5, 6]. HDACs, however, do exactly the reverse; leading to a protonated histone tail, by deacetylation of lysine amino group, that interact strongly with negatively charged DNA phosphate backbone, resulting in abnormal closed chromatin structure and transcriptional repression. The overexpression of HDACs, found in various cancers, leads to histone hypoacetylation which silences the expression of onco-suppressor genes (p53, p21, p27) [7]. HDACs, being localized in various organelles in addition to the nucleus, they regulate the chromatin structure by controlling the acetylation state of, not only histone protein, but also non-histone proteins such as tubulin, ERα, p53, HSP90, NF-γA, and GATA-1[8-13].

HDACs, thus, have a crucial role on cell cycle, cell growth, differentiation, apoptosis, immunogenicity, and angiogenesis [14] and their deregulated expression has been observed in neurological disorders [15], viral infection [16], inflammation [17] and in malignancies [18-20]. Therefore, HDACs have been identified as attractive targets for various human disorders, especially malignancies [8, 21, 22]. Many studies show that inhibition of HDAC elicits anticancer activities in several tumor cell lines [23]. HDAC inhibitors show great potential for the treatment of cancer by induction of cell cycle arrest, differentiation, and apoptosis [24-27]. To date Four HDAC-targeting drugs have been approved by FDA for treatment of

hematological malignancies. Vorinostat (soberoylanilide hydroxamic acid; SAHA, Merck, 2006) [28, 29] and Romidepsin (FK228, Gloucester Pharmaceuticals now Celgene, 2009) have been approved by FDA for treatment of cutaneous T-cell lymphoma (CTCL), Belinostat (PDX-101, TopoTarget now Onxeo, 2014) [30] has been approved for treatment of peripheral T-cell lymphoma (PTCL), and Panobinostat (LBH-589, Novartis, 2015) has been approved for multiple myeloma (MM) [29, 31-33]. In 2015, Chinese Food and Drug Administration have approved a fifth HDAC: Chidamide (Shenzhen Chipscreen Biosciences, 2015) for the treatment of PTCL. The FDA approval of these HDACIs has encouraged the development of new active molecules of the same category. Over twenty HDACIs are currently in clinical trials for targeting different cancers [34, 35]. Comparing the structures of known HDACIs like trichostatin A (TSA) and SAHA, it clearly appeared that, despite the variety of structural motifs, they share a common pharmacophore model: a metal binding functionality; in another word, zinc binding group (ZBG) acts as a chelating group for $Zn^{2+}$in the active site of HDAC, a spacer that efficiently presents the ZBG to the active site by filling the narrow tubular pocket of the enzyme. This spacer is attached to a hydrophobic terminal residue acting as surface recognition moiety called Cap via a polar connecting unit [36-41] **(Fig. 1)**. Hydroxamic acid derivatives are the broadest class of HDACIs with high affinity to HDACs, owing to the perfect chelation between hydroxamate group and $Zn^{2+}$ [42]. They inhibit HDAC at considerably lower concentrations than those considered being cytotoxic [43]. Three out of four FDA approved HDACIs are hydroxamates. This has encouraged efforts aiming at developing novel potent hydroxamate derived HDACIs with better pharmacokinetic profiles.

# Figure 1.

Encouraged by the aforementioned aspects, herein, we reported the synthesis, HDAC enzyme inhibition, and anti-proliferative activities against some tumor cell lines of two series of novel spirohydantoins and 1,2,4-triazole-3-carboxamides with the objective of designing novel and potent HDACIs **(Fig. 2)**. Two novel nuclei were introduced; 3',4'-dihydro-2'*H*-spiro[imidazolidine-4,1'-naphthalene]-2,5-dione (in

series I) and 1-(3-methoxyphenyl)-5-(3,4,5-trimethoxyphenyl)-1H-1,2,4-triazole-3-carboxamide (series II), to serve as two surface recognition moieties (Caps) to make contacts with amino acid residues at the external entrance of the HDAC active site, with the objective of comparing their effect on cytotoxicity and HDAC inhibitory activity of the synthesized compounds. To probe the impact of the linker length [44-46], six aliphatic chain spacers of variable lengths were introduced (in series I) and five spacers (in series II). Two different ZBGs; hydroxamic acid and carboxylic groups were also provided.

The structural similarities between members of series II and a series of tubulin polymerization inhibitors in our previous work [47, 48], together with the surprising and potent anti-proliferative activity of compound **9a**, have pushed us toward study the tubulin polymerization inhibitory activity of all members of series II, to demonstrate their potential activity as promising HDAC-tubulin dual inhibitors. Owing to structural similarities between (1-(3-methoxyphenyl)-5-(3,4,5-trimethoxyphenyl)-1H-1,2,4-triazole-3-carboxamide) nucleus and Combretastatin A4 (CA4) **(Fig. 2)**, in series II, the 1,2,4-triazole-3-carboxamide nucleus which was supposed to serve as a potential Cap for HDAC inhibition, was also introduced as a potential bioisostere to the *cis*-double bond of the CA4 to arrest the bioactive *cisoid* conformation.

Combretastatin A4 (CA4) is a cytotoxic agent belonging to microtubule-targeted agents. Microtubule-targeted agents (MTAs) are those agents that bind tubulin binding sites, thus, interfere with the dynamic stability of microtubules via stabilizing or destabilizing microtubule assembly. These agents act as spindle poisons leading to mitotic catastrophe, cell cycle arrest, and eventually, apoptotic cell death. CA4, in turn, belongs to the class of MTAs that destabilizes microtubules and inhibits tubulin polymerization by binding the colchicine domain of tubulin [49]. It is a potent natural anti-mitotic *cis*-stilbene derivative that was isolated by Pettit and co-workers [50-52]. It exhibits strong anti-tubulin activity and potent cytotoxicity against a variety of human cancer cell lines including those that are multidrug resistant [53, 54]. Most importantly, it has demonstrated powerful anti-angiogenesis properties [55] by altering endothelial cell structure and causing vascular permeability and rapid destruction to tumor

vasculature . It is able to elicit irreversible vascular shutdown within solid tumors leading to central tumor necrosis, leaving normal vasculature intact [56, 57]. However, its poor water solubility, low bioavailability, dose dependent toxicity [58-60], and possibility to *in vivo* convert into the more stable inactive *trans*-configuration [61] restrict its clinical application [62]. Owing to its potent anti-proliferative activity and relatively simple chemical structure, CA4 has attracted significant interest as a lead compound in the development of new anticancer analogues. Significant efforts have been done aiming at improving the pharmacokinetic profile and stabilizing the active *cis*-configuration. A prodrug of CA4; combretastatin A4 phosphate (CA4P) [63] together with a wide range of more water soluble *cis*-restricted analogues of CA4 has been identified as colchicine binding site inhibitors (CBSIs) with potent antitumor activity [64-71]. The structure-activity studies of a wide variety of CA4 analogues have demonstrated a clear view of the anticancer pharmacophore. Three preferred constituents include: a 3,4,5-trimethoxyaryl motif in ring-A, a *cis*-configured stilbene or analogous bridge retains the *cisoid* configuration linking ring-A to a 3,4-disubstituted ring-B [69, 72]. Because modifications of ring A reduce the bioactivity in most analogues of CA4 [73], ring B and the olefinic bridge offer better prospects for modification. The ring B was found to be tolerant to wide ranging of structural modification as well as the olefinic bridge which also has been subjected to substitution with different bridges in order to arrest the conformation in the *cisoid* form [74-76].

# Figure 2.

## *2. Results and Discussion*

### *2.1. Chemistry*

The designed ε-(2,5-dioxo-3',4'-dihydro-2'*H*-spiro[imidazolidine-4,1'-naphthalen]-1-yl)-*N*-hydroxyl alkanamides **5a-f** were prepared starting with one putt Bucherer-Bergs reaction [77] to afford the parent spirohydantoin (3',4'-dihydro-2'*H*-spiro[imidazolidine-4,1'-naphthalene]-2,5-dione) **2**, from α-tetralone **1**, **Scheme 1**, followed by alkylating the amidic amino group of the spirohydantoin **2** with various

ethylbromo esters to give six ethyl ester derivatives **3a-f**. Ester **3a-f** hydrolysis yielded the free acid derivatives ε-(2,5-dioxo-3',4'-dihydro-2'*H*-spiro[imidazolidine-4,1'-naphthalen]-1-yl)alkanoic acids **4a-f**, which then stirred with hydroxylamine hydrochloride in presence of *N*,*N'*-carbonyldiimidazole (CDI) [78, 79] to afford the hydroxamic acid derivatives **5a-f**.

# Scheme 1.

Procedure employed to synthesize series II involved the reaction of glycine with 3,4,5-trimethoxybenzoyl chloride in 10% sodium hydroxide to yield 2-(3,4,5-trimethoxybenzamido)acetic acid **6** [80]. Heating **6** with acetic anhydride afforded the corresponding cyclic form **7**, **Scheme 2**. The synthesis of intermediate **8** was carried out through coupling of the diazonium salt of 3-methoxyaniline with the active methylene of **7** [81]. Synthesis of the targeted compounds ε-(1-(3-methoxyphenyl)-5-(3,4,5-trimethoxyphenyl)-1*H*-1,2,4-triazole-3-carboxamido)alkanoic acids **9a-e** and -*N*-hydroxyalkanamides **10a-e** was achieved by Sawdey rearrangement reaction of **8** with five terminal amino acids to afford the acids **9a-e**, followed by stirring the acid derivatives **9a-e** with hydroxylamine hydrochloride in presence of CDI to afford the hydroxamic acid derivatives **10a-e**.

# Scheme 2.

*2.2. Biological evaluation*

*2.2.1. In vitro anti-proliferative activity*

*In vitro* anti-proliferative activity of compounds **4a-f**, **5a-f**, **9a-e**, and **10a-e**, were tested using MTT assay against two cancer cell lines as shown in **Table 1**. Results were reported as $IC_{50}$ values (in µM concentrations). Voriostat (SAHA) and CA4 were used as positive references. In series I (spirohydantoin derivatives), compounds **4a-f**, having carboxylic group as a potential ZBG, showed no anti-proliferative activity against the two tested cancer cell lines. The corresponding hydroxamic acid derivatives **5a-f** were found to be good growth inhibitors of MCF-7 cells, **Table 1**. The potency of the compounds

increased with increasing linker length **n**, which made compound **5f** the most potent growth inhibitor of MCF-7 cells in this series having $IC_{50}$ value very close to SAHA against this cancer cell line ($IC_{50}$ = 2.56 µM and 2.18 µM, for **5f** and SAHA respectively). Meanwhile, compounds **5a-f** showed low activity against HepG2 cell line. Furthermore, changing length of aliphatic linker didn't show a uniform pattern in inhibiting HepG2 cell line like that seen in case of MCF-7 cell line. For 1,2,4-triazole derivatives (series II), compounds **9a-e**, having carboxylic group as a potential ZBG, showed no anti-proliferative activity against the two tested cancer cell lines, except for the carboxylic derivative **9a** which demonstrated potent inhibition of HepG2 cells growth, with $IC_{50}$ value comparable to that of SAHA against the same cell line, and it is actually the most potent derivative of series II, **Table 1**. It also showed a moderate cytotoxic activity against MCF-7 cell line, with $IC_{50}$ value slightly lower than that of CA4. The hydroxamic acid derivatives **10a-e** showed a different pattern of anti-proliferative activity from the corresponding spirohydantoin derivatives against the two different cancer cell lines. For MCF-7 cell line they demonstrated good anti-proliferative activity, compared to CA4, but lower than SAHA. The pattern of increasing activity of **10a-e** against MCF-7 cell line was in order of decreasing linker length **n**, with the most potent derivative **10a** having 1 methylene linker. For HepG2 cell line, **10a-e** also showed good to moderate inhibitory activity, but potency increased in the order of increasing the linker length **n** and in this case the most potent derivative is **10e** having 5 methylene linker.

# Table 1.

*2.2.2. In vitro enzyme inhibition*

*2.2.2.1. In vitro HDAC inhibitory activity*

To gain insight into the mechanism of action of the synthesized compounds, compounds **5f**, **10a**, and **10e** were tested for *in vitro* HDAC inhibitory activity, $IC_{50}$ values for compounds **5f**, **10a**, and **10e** were determined against HDAC1, HDAC2, HDAC4, and HDAC6 isoforms, and SAHA was provided as a positive reference, **Table 2**. Results revealed that all tested

compounds **5f**, **10a**, and **10e** showed significant HDAC inhibitory activities against the four tested HDAC isoforms. It could be noticed that compound **5f** with spirohydantoin Cap and hexamethylene linker afforded the highest HDAC inhibitory activity with $IC_{50}$ value comparable to SAHA against HDAC4 and even lower $IC_{50}$ value in case of HDAC1. It is worth noting that, surprisingly, 10a with one methylene bridge showed considerably high HDAC inhibitory activity.

# Table 2.

*2.2.2.2. In vitro tubulin polymerization inhibitory activity*

Three members of series II; **9a**, **10a** and **10e** were tested for *in vitro* tubulin polymerization inhibitory activity in MCF-7 cells using ELISA for β-tubulin (TUBb). CA4 was employed as a positive reference, and results were reported as $IC_{50}$ values (in µM concentrations), **Table 3**. From table 3 it is noticeable that compound **9a** and CA4 afforded very close $IC_{50}$ values for TUBb inhibition. A noteworthy addition is that compound **10e** with pentamethylene bridge potently inhibited TUBb polymerization and, surprisingly, showed higher potency than CA4 ($IC_{50}$ values 4.82 and 5.73 for **10e** and CA4; respectively).

# Table 3.

*2.3. Docking studies*

Molecular modeling study was performed to investigate the mode of binding of some of the synthesized compounds. The flexible docking experiment was performed using the multistep docking protocol introduced by Koska *et al.* [82] and implemented in the Accelrys Discovery Studio 2.5 software. The obtained docked poses were ranked according to their CDocker energy ($kcal \cdot mol^{-1}$) which was

calculated at the final stage of the flexible docking protocol and was used as indication for the binding strength of the ligands [83, 84].

*2.3.1. Docking at the vorinostat binding site in HDLP (Histone Deacetylase-Like Protein)*

Molecular docking simulation of compounds **5e**, **5f**, **10a**, and **10e** into HDLP active site was done. They got stabilized at the vorinostat binding site by hydrophobic and hydrogen bond interactions, **Table 4**. It could be noticed that all the docked compounds **5e**, **5f**, **10a** and **10e** showed similar binding to vorinostat at the HDLP active site. They all showed hydrogen bonding with TYR297 as shown in vorinostat, in addition to additional bonding, listed in **Table 4**. The results of binding energies, as well as, interaction energies with HDLP were listed in **Table 4**, and revealed high CDocker energies (used as indication for the binding strength of the ligands) and CDocker interaction energies of the docked compounds. Compound **5f** showed higher CDocker energy than vorinostat which means better binding at HDLP active site (**Fig. 3**). It should be noticed that compounds **5e** and **5f** (spirohydantoin Cap) afforded much higher CDocker energies than **10a** and **10e** (1,2,4-triazole-3-carboxamide Cap), suggesting that spirohydantoin nucleus may be a better Cap for HDAC binding than 1,2,4-triazole-3-carboxamide nucleus, and these findings look consistent with HDAC inhibitory assay findings (Section (2.2.2.1)).

# Table 4.

# Figure 3.

*2.3.2. Docking at the colchicine binding site in tubulin protein*

Compounds **9a**, **10a**, **10e** and CA4 were docked into the colchicine binding site buried between α-tubulin and β-tubulin mainly in the β subunit. The X-ray crystallographic structure of DAMA colchicine-tubulin complex (PDB (www.rcsb.org) code 1SA0) was used as the tubulin protein template. Molecular docking simulation of compounds **9a**, **10a** and **10e** into tubulin protein binding site was done. They got stabilized at the colchicine-binding site of tubulin by hydrophobic and hydrogen bond interactions (types of interactions were listed in **Table 5**). The results of

binding energies, as well as, interaction energies with tubulin protein were listed in **Table 5**, and revealed high CDocker energies and CDocker interaction energies of the docked compounds. Compound **9a** and **10a** afforded almost the same CDocker energies as CA4. Meanwhile, compound **10e** afforded higher CDocker energy than CA4 indicating better binding of **10e** at the colchicine binding site. It should be noticed that there is an extra hydrogen bond between hydroxamate moiety of **10e** and GTP in the binding site, and these findings are in agreement with the results of tubulin inhibition assay (Section 2.2.2.2). These results reflect the importance of the carboxylate or hydroxamate groups separated from the 1,2,4-triazole group by one or more methylene group in holding the molecule at place (binding) at the active site by extra hydrogen bonds and justifies the experimental findings (Section 2.2.2). These findings may be fruitful in designing compounds of better tubulin polymerization inhibition than CA4. [85]

# Table 5.

*2.4. Drug likeliness and oral bioavailability*

The increase in molecular weight of the deigned compounds is still in an acceptable range.

- Reports suggest that oral bioavailability is mainly affected by 3 different criteria; 1- no more than 10 rotatable bonds in the specified compound 2- 12 or fewer H bond donors and acceptors, 3- the compound have a polar surface area (PSA) of 140 $A^2$ or less [86].

# Table 6.

From the above table we can suggest that the designed compounds are orally available. They have only 4 HBA and 3 donors. The polar surface area measured did not exceed 140 $A^2$. Only compound **10e** exceeded the 500 dalton rule in Lipiniski's but this is the only violation to the rule, also the 500 molecular weight cutoff has been questioned. Polar surface area and the number of rotatable bonds has been found to better discriminate between compounds that are orally active and those that are

not for a large data set of compounds in the ratio with number of HBD and acceptors (12) and PSA (124). Log P, all compounds in an acceptable range (the accepted range is 0.4-5.6).

*3. Conclusion*

Two novel series of spirohydantoins and 1,2,4-triazole-3-carboxamide derivatives were successfully designed, synthesized, evaluated for their anti-proliferative activity as well as enzyme inhibitory activity. Molecular modeling study was performed to assess the potential binding ability of some compounds to HDAC enzyme as well as the colchicine binding site of β-tubulin. Results of anti-proliferative activity, tubulin and HDAC enzyme inhibitory activities, as well as docking simulation results of tested compounds were found to be consistent with each other in a reasonable way, and they confirmed the following; For series I, introduction of the spirohydantoin nucleus (3',4'-dihydro-2'*H*-spiro[imidazolidine-4,1'-naphthalene]-2,5-dione) as a new Cap for HDAC binding is successful. Linking this Cap to a hydroxamic moiety as a ZBG looks essential for activity of these derivatives, as the corresponding carboxylic derivatives devoided from any cytotoxic activity against the tested cell lines. Aliphatic linkers of various lengths affect the anti-proliferative activity together with HDAC inhibitory activity of compounds; the potency against MCF-7 cell line increase, in an ascending pattern, with increasing methylene bridge length **n**, reaching the highest activity with hexamethylene bridge in compound **5f**, which also showed a remarkable inhibition of HDAC comparable to SAHA (Sections (2.2.2) and (2.3.1)). The involvement of HDAC inhibition as a possible mechanism of action is confirmed from *in vitro* HDAC inhibitory assay as well as docking at HDLP active site. For series II, the nucleus (1-(3-methoxyphenyl)-5-(3,4,5-trimethoxyphenyl)-1*H*-1,2,4-triazole-3-carboxamide) is found to be a successful Cap for HDAC binding, as well as, a good CA4 analogous moiety for tubulin inhibition (sections (2.2.2) and (2.3.2)). The lack of anti-proliferative activity in compounds **9b-e** suggests the importance of a small linker (one methylene bridge) for the activity of carboxylic derivatives as seen from the great variation between the activity of **9a** and the rest of members **9b-e** against HepG2 cell line. For hydroxamic acid derivatives **10a-e**, aliphatic linkers of variable lengths affect the anti-proliferative

activity as follows; for MCF-7 cell line, the pattern of increasing activity of **10a-e** was in order of decreasing linker length (**n)**. These results are in agreement with results of previous studies introducing HDAC-tubulin dual acting entities on the same cell line (MCF-7) [44]. Meanwhile, for HepG2 cell line, potency of **10a-e** increased in the order of increasing the linker length **(n)**, which goes in line with HDAC and tubulin inhibitory findings, as well as docking results. The previous findings suggests that, the possible mechanisms explaining the cytotoxic actions of the series II derivatives **10a-e** might involve both HDAC inhibition, in addition to tubulin polymerization inhibition activities. Comparing the results of spirohydantoin derivatives **5a-f** versus 1,2,4-triazole derivatives **10a-e**, the higher HDAC inhibition shown for spirohydantoin series **5a-f** suggests that spirohydantoin nucleus may act as a better Cap for HDAC binding than 1,2,4-triazole-3-carboxamide nucleus. Meanwhile, the higher anti-proliferative activities of **10a-e** than **5a-e** suggest involvement of another mechanism of action for 1,2,4-triazole derivatives, which might be tubulin polymerization inhibition.

## 4. *Experimental*

### *4.1. Chemistry*

Chemicals and solvents used were of analytical grade. Reaction progression was routinely monitored by thin-layer chromatography (TLC) on Merck 9385 pre-coated aluminum plate silica gel (Kieselgel 60) 5 x 20 cm plates with a layer thickness of 0.2 mm, and spots were visualized by exposure to UV-lamp at $\lambda$ = 254 nm. Melting points were determined on Stuart electro-thermal melting point apparatus and were uncorrected. IR spectra were recorded on Nicolet iS5 (ATR) FT-IR spectrometer, Faculty of Pharmacy, Minia University. $^{1}$H NMR spectra were carried out using Bruker apparatus 400 MHz spectrometer, Faculty of Pharmaceutical sciences, The University of British Columbia, Canada, using DMSO-$d_6$ (2.5) as a solvent. $^{13}$C NMR spectra were carried out using Bruker apparatus 100 MHz spectrometer, Faculty of Science, Western University, Canada, using DMSO-$d_6$ (39.51) as a solvent. High resolution mass spectra (HRMS) were obtained on a Thermo Scientific Q Exactive™ Orbitrap mass spectrometer, Faculty of Pharmaceutical sciences, The University of British Columbia, Canada.

*4.1.1. 3',4'-dihydro-2'H-spiro[imidazolidine-4,1'-naphthalene]-2,5-dione **2*** [87]. Yellowish white solid (1.44 g, 66.67% yield); mp 239-41 °C; reported 241-2.5 °C.

*4.1.2. General procedure for the synthesis of compounds **3a-f***. To a solution of the spirohydantoin **2** (0.01 mol, 2.16 g) in dry acetone (90 mL), anhydrous potassium carbonate (0.02 mol, 2.76 g) and the appropriate bromoester (0.01 mol) were added. The reaction mixture was stirred under reflux for 6 h, the solvent was then distilled off under reduced pressure, and the reaction mixture was diluted with ice water. The precipitate formed was filtered off, washed with water, and dried to give the corresponding ester.

*4.1.2.1. Ethyl 2-(2,5-dioxo-3',4'-dihydro-2'H-spiro[imidazolidine-4,1'-naphthalen]-1-yl) acetate **3a*** [88]. Reaction of **2** with ethyl bromoacetate yielded pale yellow powder (1.96 g, 64.90% yield); mp 130-2°C; reported 133-135°C.

*4.1.2.2. Ethyl 3-(2,5-dioxo-3',4'-dihydro-2'H-spiro[imidazolidine-4,1'-naphthalen]-1-yl) propionate **3b***. Reaction of **2** with ethyl 3-bromopropionate yielded pale yellow powder (1.92 g, 60.76%); mp 161-2°C; IR ($cm^{-1}$): 3317 (NH), 1771 (C=O), 1751 (C=O), 1704 (C=O), 1190 (C-O); $^1$H NMR (400 MHz, DMSO-$d_6$) δ (ppm): 1.18 (t, 3H, *J* = 7.20 Hz, $CH_2$-C<u>H</u>$_3$), 1.82-1.93 (m, 2H, $CH_2$-cyclohexane), 2.06 (t, 2H, *J* = 8.01 Hz, $CH_2$-cyclohexane), 2.64 (t, 2H, *J* = 6.80 Hz, C<u>H</u>$_2$-CO), 2.79 (t, 2H, *J* = 8.01 Hz, $CH_2$-cyclohexane), 3.69 (t, 2H, *J* = 6.80 Hz, N-C<u>H</u>$_2$), 4.05 (q, 2H, *J* = 7.20 Hz, O-C<u>H</u>$_2$-$CH_3$), 7.04 (d, 1H, *J* = 8.00 Hz, Ar-H), 7.17 (d, 2H, *J* = 8.00 Hz, 2 Ar-H), 7.24 (d, 1H, *J* = 8.00 Hz, Ar-H), 8.86 (s, 1H, N<u>H</u>); HRMS: m/z calculated for $C_{17}H_{20}N_2O_4[M-H]^+$: 315.13503, found: 315.13538.

*4.1.2.3. Ethyl 4-(2,5-dioxo-3',4'-dihydro-2'H-spiro[imidazolidine-4,1'-naphthalen]-1-yl) butyrate **3c***. Reaction of **2** with ethyl 4-bromobutyrate yielded pale yellow powder (2.24 g, 67.87%); mp 172-4°C; IR ($cm^{-1}$): 3309 (NH), 1771 (C=O), 1748 (C=O), 1707 (C=O), 1190 (C-O); $^1$H NMR (400 MHz, DMSO-$d_6$) δ (ppm): 1.19 (t, 3H, *J* = 7.20 Hz, $CH_2$-C<u>H</u>$_3$), 1.80-1.84 (m, 2H, C<u>H</u>$_2$-$CH_2$-CO), 1.92-1.94 (m, 2H, $CH_2$-cyclohexane), 2.08 (t, 2H, *J* = 7.20 Hz, $CH_2$-cyclohexane), 2.34 (t, 2H, *J* = 6.80 Hz, C<u>H</u>$_2$-CO), 2.79 (t, 2H, *J* = 7.20 Hz, $CH_2$-cyclohexane), 3.47 (t, 2H, *J* = 6.80 Hz, N-C<u>H</u>$_2$), 4.06 (q, 2H, *J* = 7.20 Hz, O-C<u>H</u>$_2$-

$CH_3$), 6.99 (d, 1H, *J* = 8.00 Hz, Ar-H), 7.19 (d, 2H, *J* = 8.00 Hz, 2 Ar-H), 7.24 (d, 1H, *J* = 8.00 Hz, Ar-H), 8.83 (br s, 1H, NH); HRMS: m/z calculated for $C_{18}H_{22}N_2O_4[M-H]^+$: 329.15068, found: 329.15054.

*4.1.2.4. Ethyl 5-(2,5-dioxo-3',4'-dihydro-2'H-spiro[imidazolidine-4,1'-naphthalen]-1-yl) pentanoate* ***3d***. Reaction of **2** with ethyl 5-bromovalerate yielded pale yellow powder (2.12 g, 61.62%); mp 156-7°C; IR ($cm^{-1}$): 3306 (NH), 1771 (C=O), 1753 (C=O), 1700 (C=O), 1207 (C-O); $^1$H NMR (400 MHz, DMSO-$d_6$) δ (ppm): 1.17 (t, 3H, *J* = 6.80 Hz, $CH_2$-$CH_3$), 1.52-1.57 (m, 4H, $CH_2$-$CH_2$-$CH_2$-CO), 1.82-1.94 (m, 2H, $CH_2$-cyclohexane), 2.07 (t, 2H, *J* = 6.40 Hz, $CH_2$-cyclohexane), 2.34 (t, 2H, *J* = 7.20 Hz, $CH_2$-CO), 2.79 (t, 2H, *J* = 6.40 Hz, $CH_2$-cyclohexane), 3.43 (t, 2H, *J* = 7.20 Hz, N-$CH_2$), 4.05 (q, 2H, *J* = 6.80 Hz, O-$CH_2$-$CH_3$), 6.99 (d, 1H, *J* = 8.00 Hz, Ar-H), 7.18 (d, 2H, *J* = 8.00 Hz, 2 Ar-H), 7.25 (d, 1H, *J* = 8.00 Hz, Ar-H), 8.83 (br s, 1H, NH); HRMS: m/z calculated for $C_{19}H_{24}N_2O_4[M-H]^+$: 343.16633, found: 343.16595.

*4.1.2.5. Ethyl 6-(2,5-dioxo-3',4'-dihydro-2'H-spiro[imidazolidine-4,1'-naphthalen]-1-yl) hexanoate* ***3e***. Reaction of **2** with ethyl 6-bromohexanoate yielded pale yellow powder (2.20 g, 61.45%); mp 143-5°C; IR ν ($cm^{-1}$): 3306 (NH), 1771 (C=O), 1753 (C=O), 1700 (C=O), 1177 (C-O); $^1$H NMR (400 MHz, DMSO-$d_6$) δ (ppm): 1.16 (t, 3H, *J* = 7.20 Hz, $CH_2$-$CH_3$), 1.25-1.30 (m, 2H, $CH_2$-$CH_2$-$CH_2$-CO), 1.56-1.59 (m, 4H, $CH_2$-$CH_2$-$CH_2$-$CH_2$-CO), 1.80-1.93 (m, 2H, $CH_2$-cyclohexane), 2.08 (t, 2H, *J* = 6.40 Hz, $CH_2$-cyclohexane), 2.29 (t, 2H, *J* = 7.20 Hz, $CH_2$-CO), 2.79 (t, 2H, *J* = 6.40 Hz, $CH_2$-cyclohexane), 3.41 (t, 2H, *J* = 7.20 Hz, N-$CH_2$), 4.06 (q, 2H, *J* = 7.20 Hz, O-$CH_2$-$CH_3$), 6.97 (d, 1H, *J* = 7.20 Hz, Ar-H), 7.19 (d, 2H, *J* = 7.20 Hz, 2 Ar-H), 7.24 (d, 1H, *J* = 7.20 Hz, Ar-H), 8.80 (br s, 1H, NH); HRMS: m/z calculated for $C_{20}H_{26}N_2O_4[M-H]^+$: 357.18198, found: 357.18216.

*4.1.2.6. Ethyl 7-(2,5-dioxo-3',4'-dihydro-2'H-spiro[imidazolidine-4,1'-naphthalen]-1-yl) heptanoate* ***3f***. Reaction of **2** with ethyl 7-bromoheptanoate yielded pale yellow powder (2.30 g, 61.82%); mp 162-3°C; IR ν ($cm^{-1}$): 3306 (NH), 1772 (C=O), 1751 (C=O), 1703 (C=O), 1189 (C-O); $^1$H NMR (400 MHz, DMSO-$d_6$) δ (ppm): 1.15-1.17 (m, 2H, $CH_2$-$CH_2$-$CH_2$-CO), 1.20 (t, 3H, *J* = 6.80 Hz, $CH_2$-$CH_3$), 1.25-1.29 (m, 2H, N-$CH_2$-$CH_2$-$CH_2$), 1.56-1.59 (m, 4H, $CH_2$-$CH_2$-$CH_2$-$CH_2$-$CH_2$-CO), 1.82-1.93 (m, 2H,

$CH_2$-cyclohexane), 2.08 (t, 2H, *J* = 7.20 Hz, $CH_2$-cyclohexane), 2.28 (t, 2H, *J* = 7.20 Hz, C$\underline{H_2}$-CO), 2.79 (t, 2H, *J* = 7.20 Hz, $CH_2$-cyclohexane), 3.41 (t, 2H, *J* = 7.20 Hz, N-C$\underline{H_2}$), 4.06 (q, 2H, *J* = 6.80 Hz, O-C$\underline{H_2}$-$CH_3$), 6.97 (d, 1H, *J* = 7.80 Hz, Ar-H), 7.20 (d, 2H, *J* = 7.80 Hz, 2 Ar-H), 7.24 (d, 1H, *J* = 7.80 Hz, Ar-H), 8.82 (br s, 1H, N$\underline{H}$); HRMS: m/z calculated for $C_{21}H_{28}N_2O_4[M-H]^+$: 371.19887, found: 371.19977.

*4.1.3. General procedure for the synthesis of compounds **4a-f***

General procedure for the synthesis of compounds **4a-f** [89].

*4.1.3.1. 2-(2,5-Dioxo-3',4'-dihydro-2'H-spiro[imidazolidine-4,1'-naphthalen]-1-yl)acetic acid **4a*** [88]. Yellowish white powder (3.50 g, 51.10% yield); mp 228-29°C; reported 231-3°C.

*4.1.3.2. 3-(2,5-Dioxo-3',4'-dihydro-2'H-spiro[imidazolidine-4,1'-naphthalen]-1-yl)propionic acid* **4b**. Yellowish white powder (3.70 g, 51.40% yield); mp 240-1°C; IR ν ($cm^{-1}$): 3675-2570 (OH), 3306 (NH), 1769 (C=O), 1706 (C=O), 1690 (C=O); $^1$H NMR (400 MHz, DMSO-$d_6$) δ (ppm): 1.83-1.93 (m, 2H, $CH_2$-cyclohexane), 2.06 (t, 2H, *J* = 7.20 Hz, $CH_2$-cyclohexane), 2.58 (t, 2H, *J* = 8.01 Hz, C$\underline{H_2}$-CO), 2.79 (t, 2H, *J* = 7.20 Hz, $CH_2$-cyclohexane), 3.66 (t, 2H, *J* = 8.01 Hz, N-C$\underline{H_2}$), 7.06 (d, 1H, *J* = 7.80 Hz, Ar-H), 7.18 (d, 2H, *J* = 7.80 Hz, 2 Ar-H), 7.23 (d, 1H, *J* = 7.80 Hz, Ar-H), 8.84 (s, 1H, N$\underline{H}$), 12.39 (br s, 1H, O$\underline{H}$); $^{13}$C NMR (100 MHz, DMSO-$d_6$) δ (ppm): 176.4, 162.3, 155.9, 138.2, 134.5., 129.6, 128.5, 127.3, 126.9, 62.3, 34.6, 33.9, 32.5, 28.9, 18.8; HRMS: m/z calculated for $C_{15}H_{16}N_2O_4[M-H]^+$: 287.10373, found: 287.10397.

*4.1.3.3. 4-(2,5-Dioxo-3',4'-dihydro-2'H-spiro[imidazolidine-4,1'-naphthalen]-1-yl)butyric acid* **4c**. Yellowish white powder (3.85 g, 51% yield); mp 249-51°C; IR ν ($cm^{-1}$): 3670-2550 (OH), 3322 (NH), 1765 (C=O), 1705 (C=O), 1690 (C=O); $^1$H NMR (400 MHz, DMSO-$d_6$) δ (ppm): 1.81-1.85 (m, 2H, $\underline{CH_2}$-$CH_2$-CO), 1.89-1.94 (m, 2H, $CH_2$-cyclohexane), 2.09 (t, 2H, *J* = 7.20 Hz, $CH_2$-cyclohexane), 2.26 (t, 2H, *J* = 6.80 Hz, C$\underline{H_2}$-CO), 2.79 (t, 2H, *J* = 7.20 Hz, $CH_2$-cyclohexane), 3.46 (t, 2H, *J* = 6.80 Hz, N-C$\underline{H_2}$), 6.99 (d, 1H, *J* = 6.40 Hz, Ar-H), 7.19 (d, 2H, *J* = 6.40 Hz, 2 Ar-H), 7.25 (d, 1H, *J* = 6.40 Hz, Ar-H), 8.83 (s, 1H, N$\underline{H}$),12.11 (br s, 1H, O$\underline{H}$); $^{13}$C NMR (100 MHz, DMSO-$d_6$) δ (ppm): 176.7, 174.1,

156.3, 138.3, 134.5, 129.7, 128.5, 127.0, 126.9, 62.3, 37.8, 33.9, 31.3, 28.9, 23.6, 18.8; HRMS: m/z calculated for $C_{16}H_{18}N_2O_4[M-H]^+$: 301.11938, found: 301.11938.

*4.1.3.4. 5-(2,5-Dioxo-3',4'-dihydro-2'H-spiro[imidazolidine-4,1'-naphthalen]-1-yl)pentanoic acid* ***4d***. Yellowish white powder (4.02 g, 50.88% yield); mp 260-1°C; IR ($cm^{-1}$): 3665-2560 (OH), 3400 (NH), 1766 (C=O), 1711 (C=O), 1700 (C=O); $^1$H NMR (400 MHz, DMSO-$d_6$) δ (ppm): 1.56-1.58 (m, 4H, C$\underline{H_2}$-C$\underline{H_2}$-CH$_2$-CO), 1.88-1.93 (m, 2H, CH$_2$-cyclohexane), 2.08 (t, 2H, *J* = 6.80 Hz, CH$_2$-cyclohexane), 2.26 (t, 2H, *J* = 7.80 Hz, C$\underline{H_2}$-CO), 2.78 (t, 2H, *J* = 6.80 Hz, CH$_2$-cyclohexane), 3.42 (t, 2H, *J* = 7.80 Hz, N-C$\underline{H_2}$), 6.99 (d, 1H, *J* = 8.00 Hz, Ar-H), 7.18 (d, 2H, *J* = 8.00 Hz, 2 Ar-H), 7.24 (d, 1H, *J* = 8.00 Hz, Ar-H), 8.83 (s, 1H, N$\underline{H}$), 12.03 (br s, 1H, O$\underline{H}$); $^{13}$C NMR (100 MHz, DMSO-$d_6$) δ (ppm): 177.9, 174.3, 157.5, 139.5, 135.8, 131.0, 129.7, 128.2, 63.5, 39.1, 35.3, 34.5, 30.1, 28.7, 23.3, 15.8; HRMS: m/z calculated for $C_{17}H_{20}N_2O_4[M-H]^+$: 315.13503, found: 315.13531.

*4.1.3.5. 6-(2,5-Dioxo-3',4'-dihydro-2'H-spiro[imidazolidine-4,1'-naphthalen]-1-yl)hexanoic acid* ***4e***. Yellowish white powder (4.20 g, 50.90% yield); mp 275-7°C; IR ($cm^{-1}$): 3678-2575 (OH), 3348 (NH), 1764 (C=O), 1711 (C=O), 1698 (C=O); $^1$H NMR (400 MHz, DMSO-$d_6$) δ (ppm): 1.24-1.29 (m, 2H, C$\underline{H_2}$-CH$_2$-CH$_2$-CO), 1.51-1.59 (m, 4H, C$\underline{H_2}$-CH$_2$-C$\underline{H_2}$-CH$_2$-CO), 1.82-1.94 (m, 2H, CH$_2$-cyclohexane), 2.07 (t, 2H, *J* = 6.80 Hz, CH$_2$-cyclohexane), 2.21 (t, 2H, *J* = 7.80 Hz, C$\underline{H_2}$-CO), 2.78 (t, 2H, *J* = 6.80 Hz, CH$_2$-cyclohexane), 3.42 (t, 2H, *J* = 7.20 Hz, N-C$\underline{H_2}$), 6.98 (d, 1H, *J* = 7.80 Hz, Ar-H), 7.20 (d, 2H, *J* = 7.80 Hz, 2 Ar-H), 7.24 (d, 1H, *J* = 7.80 Hz, Ar-H), 8.82 (s, 1H, NH), 11.94 (br s, 1H, OH); $^{13}$C NMR (100 MHz, DMSO-$d_6$) δ (ppm): 176.7, 174.7, 156.3, 138.2, 134.5, 129.7, 128.4, 127.3, 126.9, 62.2, 38.1, 34.0, 33.9, 28.9, 27.7, 26.1, 24.5, 18.9; HRMS: m/z calculated for $C_{18}H_{22}N_2O_4[M-H]^+$: 329.15068, found: 329.15088.

*4.1.3.6. 7-(2,5-Dioxo-3',4'-dihydro-2'H-spiro[imidazolidine-4,1'-naphthalen]-1-yl)heptanoic acid* ***4f***. Yellowish white powder (4.43 g, 51.51% yield); mp 284-6°C; IR ($cm^{-1}$): 3675-2550 (OH), 3335 (NH), 1769 (C=O), 1708 (C=O), 1698 (C=O); $^1$H NMR (400 MHz, DMSO-$d_6$) δ (ppm): 1.18-1.22 (m, 2H, C$\underline{H_2}$-CH$_2$-CH$_2$-CO), 1.27-1.30 (m, 2H, N-CH$_2$-CH$_2$-C$\underline{H_2}$), 1.52-1.59 (m, 4H, C$\underline{H_2}$-CH$_2$-CH$_2$-C$\underline{H_2}$-CH$_2$-

CO), 1.82-1.94 (m, 2H, $CH_2$-cyclohexane), 2.08 (t, 2H, *J* = 6.80 Hz, $CH_2$-cyclohexane), 2.23 (t, 2H, *J* = 7.20 Hz, C$\underline{H_2}$-CO), 2.78 (t, 2H, *J* = 6.80 Hz, $CH_2$-cyclohexane), 3.41 (t, 2H, *J* = 7.20 Hz, N-C$\underline{H_2}$), 6.97 (d, 1H, *J* = 7.20 Hz, Ar-H), 7.19 (d, 2H, *J* = 7.20 Hz, 2 Ar-H), 7.25 (d, 1H, *J* = 7.20 Hz, Ar-H) 8.83 (s, 1H, NH), 11.96 (br s, 1H, OH); $^{13}$C NMR (100 MHz, DMSO-$d_6$) δ (ppm): 177.9, 174.2, 156.3, 138.2, 135.2, 129.7, 128.4, 126.9 126.8, 62.2, 38.2, 34.0, 28.8, 28.5, 27.8, 26.2, 25.6, 25.5, 18.6; HRMS: m/z calculated for $C_{19}H_{24}N_2O_4[M-H]^+$: 343.17088, found: 343.17090.

*4.1.4. General procedure for the synthesis of compounds **5a-f***. The acid **4** (0.01 mol) was dissolved in tetrahydrofuran (THF, 10 mL), *N,N'*-carbonyldiimidazole (CDI, 0.04 mol, 6.48 g) was added at 25-30°C and stirred for 1 h. Hydroxylamine hydrochloride (0.04 mol, 2.78 g) was added, and the stirring was continued for another 1 h. The solvent was distilled off, ethylacetate (10 mL) was added, washed with water (2 x 10 mL), and the organic layer was collected, dried over anhydrous sodium sulphate, filtered, and evaporated under vacuum. The product was collected as oily droplets.

*4.1.4.1. 2-(2,5-Dioxo-3',4'-dihydro-2'H-spiro[imidazolidine-4,1'-naphthalen]-1-yl)-N-hydroxyacetamide **5a***. Yellowish brown oil (1.46 g, 50.52% yield); IR (cm$^{-1}$): 3401 (OH), 3360 (NH), 3306 (NH), 1777 (C=O), 1706 (C=O), 1698 (C=O); $^1$H NMR (400 MHz, DMSO-$d_6$) δ (ppm): 1.95-1.97 (m, 2H, $CH_2$-cyclohexane), 2.09 (t, 2H, *J* = 7.20 Hz, $CH_2$-cyclohexane), 2.79 (t, 2H, *J* = 7.20 Hz, $CH_2$-cyclohexane), 4.14 (s, 2H, N- C$\underline{H_2}$-CO), 7.07 (d, 1H, *J* = 8.00 Hz, Ar-H), 7.19 (d, 2H, *J* = 8.00 Hz, 2 Ar-H), 7.25 (d, 1H, *J* = 8.00 Hz, Ar-H), 8.99 (s, 1H, NH), 11.20 (br s, 2H, NHOH); $^{13}$C NMR (100 MHz, DMSO-$d_6$) δ (ppm): 176.4, 169.3, 155.5, 138.2, 134.4, 129.6, 128.5, 127.6, 126.9, 62.8, 40.8, 34.0, 28.8, 18.8; HRMS: m/z calculated for $C_{14}H_{15}N_3O_4[M-H]^+$: 288.10923, found: 288.10935.

*4.1.4.2. 3-(2,5-Dioxo-3',4'-dihydro-2'H-spiro[imidazolidine-4,1'-naphthalen]-1-yl)-N-hydroxypropionamide **5b***. Yellowish brown oil (1.51 g, 49.83% yield); IR (cm$^{-1}$): 3400 (OH), 3362 (NH), 3305 (NH), 1778 (C=O), 1705 (C=O), 1697 (C=O); $^1$H NMR (400 MHz, DMSO-$d_6$) δ (ppm): 1.85-1.93 (m, 2H, $CH_2$-cyclohexane), 2.07 (t, 2H, *J* = 6.80 Hz, $CH_2$-cyclohexane), 2.58 (t, 2H, *J* = 7.20 Hz, C$\underline{H_2}$-CO), 2.78 (t, 2H, *J* = 6.80 Hz, $CH_2$-cyclohexane), 3.66 (t, 2H, *J* = 7.20 Hz, N-C$\underline{H_2}$), 7.06 (d,

1H, *J* = 6.40 Hz, Ar-H), 7.17 (d, 2H, , *J* = 6.40 Hz, 2 Ar-H), 7.23 (d, 1H, , *J* = 6.40 Hz, Ar-H), 8.84 (s, 1H, NH), 11.50 (br s, 2H, NHOH); $^{13}$C NMR (100 MHz, DMSO-$d_6$) δ (ppm): 176.4, 169.7, 155.9, 138.2, 134.5., 129.6, 128.5, 127.3, 126.9, 63.5, 34.6, 33.9, 32.5, 28.9, 18.8; HRMS: m/z calculated for $C_{15}H_{17}N_3O_4[M-H]^+$: 302.11963, found: 302.11985.

*4.1.4.3. 4-(2,5-Dioxo-3',4'-dihydro-2'H-spiro[imidazolidine-4,1'-naphthalen]-1-yl)-N-hydroxybutyramide* ***5c***. Pale brown oil (1.53 g, 48.26% yield); IR (cm$^{-1}$): 3402 (OH), 3365 (NH), 3302 (NH), 1777 (C=O), 1707 (C=O), 1697 (C=O); $^1$H NMR (400 MHz, DMSO-$d_6$) δ (ppm): 1.81-1.85 (m, 2H, C$\underline{H_2}$-CH$_2$-CO), 1.89-1.94 (m, 2H, CH$_2$-cyclohexane), 2.09 (t, 2H, *J* = 6.80 Hz, CH$_2$-cyclohexane), 2.26 (t, 2H, *J* = 7.20 Hz, C$\underline{H_2}$-CO), 2.80 (t, 2H, *J* = 6.80 Hz, CH$_2$-cyclohexane), 3.46 (t, 2H, *J* = 7.20 Hz, N-C$\underline{H_2}$), 6.99 (d, 1H, *J* = 8.00 Hz, Ar-H), 7.19 (d, 2H, *J* = 8.00 Hz, 2 Ar-H), 7.25 (d, 1H, *J* = 8.00 Hz, Ar-H), 8.83 (s, 1H, NH), 11.30 (br s, 2H, NHOH); $^{13}$C NMR (100 MHz, DMSO-$d_6$) δ (ppm): 174.1, 162.3, 156.3, 138.3, 134.5, 129.7, 128.5, 127.0, 126.9, 62.4, 37.8, 33.9, 31.4, 28.9, 23.6, 18.8; HRMS: m/z calculated for $C_{16}H_{19}N_3O_4[M-H]^+$: 316.13811, found: 316.13902.

*4.1.4.4. 5-(2,5-Dioxo-3',4'-dihydro-2'H-spiro[imidazolidine-4,1'-naphthalen]-1-yl)-N-hydroxypentanamide* ***5d***. Pale brown oil (1.71 g, 51.66% yield); IR (cm$^{-1}$): 3404 (OH), 3367 (NH), 3306 (NH), 1778 (C=O), 1707 (C=O), 1699 (C=O); $^1$H NMR (400 MHz, DMSO-$d_6$) δ (ppm): 1.56-1.58 (m, 4H, C$\underline{H_2}$-C$\underline{H_2}$-CH$_2$-CO), 1.88-1.93 (m, 2H, CH$_2$-cyclohexane), 2.07 (t, 2H, *J* = 6.80 Hz, CH$_2$-cyclohexane), 2.26 (t, 2H, *J* = 7.20 Hz, C$\underline{H_2}$-CO), 2.79 (t, 2H, *J* = 6.80 Hz, CH$_2$-cyclohexane), 3.43 (t, 2H, *J* = 7.20 Hz, N-C$\underline{H_2}$), 6.99 (d, 1H, *J* = 8.00 Hz, Ar-H), 7.18 (d, 2H, *J* = 8.00 Hz, 2 Ar-H), 7.24 (d, 1H, *J* = 8.00 Hz, Ar-H), 8.83 (s, 1H, NH), 11.25 (br s, 2H, NHOH); $^{13}$C NMR (100MHz, DMSO-$d_6$) δ (ppm): 174.4, 169.3, 157.4, 139.5, 135.7, 131.0, 129.7, 128.2, 63.5, 38.9, 35.3, 34.5, 30.1, 28.8, 23.3, 15.9; HRMS: m/z calculated for $C_{17}H_{21}N_3O_4[M-H]^+$: 330.14883, found: 330.14903.

*4.1.4.5. 6-(2,5-Dioxo-3',4'-dihydro-2'H-spiro[imidazolidine-4,1'-naphthalen]-1-yl)-N-hydroxyhexanamide* ***5e***. Pale brown oil (1.75 g, 50.72% yield); IR (cm$^{-1}$): 3407 (OH), 3367 (NH), 3306 (NH), 1778 (C=O), 1708 (C=O), 1699 (C=O); $^1$H NMR (400 MHz, DMSO-$d_6$) δ (ppm): 1.26-1.29 (m,

2H, C$\underline{H_2}$-$CH_2$-$CH_2$-CO), 1.53-1.60 (m, 4H, C$\underline{H_2}$-$CH_2$-C$\underline{H_2}$-$CH_2$-CO), 1.82-1.94 (m, $CH_2$-cyclohexane), 2.07 (t, 2H, *J* = 6.80 Hz, $CH_2$-cyclohexane), 2.26 (t, 2H, *J* = 7.20 Hz, C$\underline{H_2}$-CO), 2.79 (t, 2H, *J* = 6.80 Hz, $CH_2$-cyclohexane), 3.41 (t, 2H, *J* = 7.20 Hz, N-C$\underline{H_2}$), 6.97 (d, 1H, *J* = 7.00 Hz, Ar-H), 7.19 (d, 2H, *J* = 7.00 Hz, 2 Ar-H), 7.23 (d, 1H, *J* = 7.00 Hz, Ar-H), 8.82 (s, 1H, NH), 11.46 (br s, 2H, NHOH); $^{13}$C NMR (100 MHz, DMSO-$d_6$) δ (ppm): 174.7, 169.4, 156.5, 138.4, 134.5, 129.7, 128.4, 127.3, 126.9, 62.3, 38.3, 34.0, 33.9, 28.8, 27.7, 26.1, 24.3, 18.9; HRMS: m/z calculated for $C_{18}H_{23}N_3O_4[M-H]^+$: 344.16158, found: 344.16301.

*4.1.4.6. 7-(2,5-Dioxo-3',4'-dihydro-2'H-spiro[imidazolidine-4,1'-naphthalen]-1-yl)-N-hydroxyheptanamide* ***5f***. Pale brown oil (4.43 g, 51.51% yield); IR ($cm^{-1}$): 3402 (OH), 3365 (NH), 3302 (NH), 1777 (C=O), 1707 (C=O), 1697 (C=O); $^1$H NMR (400 MHz, DMSO-$d_6$) δ (ppm): 1.19-1.22 (m, 2H, C$\underline{H_2}$-$CH_2$-$CH_2$-CO), 1.27-1.30 (m, 2H, N-$CH_2$-$CH_2$-C$\underline{H_2}$), 1.52-1.60 (m, 4H, C$\underline{H_2}$-$CH_2$-$CH_2$-C$\underline{H_2}$-$CH_2$-CO), 1.82-1.94 (m, 2H, $CH_2$-cyclohexane), 2.07 (t, 2H, *J* = 6.80 Hz, $CH_2$-cyclohexane), 2.21 (t, 2H, *J* = 7.20 Hz, C$\underline{H_2}$-CO), 2.78 (t, 2H, *J* = 6.80 Hz, $CH_2$-cyclohexane), 3.42 (t, 2H, *J* = 7.20 Hz, N-C$\underline{H_2}$), 6.98 (d, 1H, *J* = 6.40 Hz, Ar-H), 7.20 (d, 2H, *J* = 6.40 Hz, 2 Ar-H), 7.24 (d, 1H, *J* = 6.40 Hz, Ar-H) 8.82 (s, 1H, NH), 11.17 (br s, 2H, NHOH); $^{13}$C NMR (100 MHz, DMSO-$d_6$) δ (ppm): 176.7, 169.7, 156.3, 138.3, 135.1, 129.7, 128.4, 126.9 126.8, 62.2, 38.1, 34.0, 28.8, 28.5, 27.8, 26.3, 25.6, 25.5, 18.8; HRMS: m/z calculated for $C_{19}H_{25}N_3O_4[M-H]^+$: 358.17723, found: 358.17920.

*4.1.5. 4-(2-(3-methoxyphenyl)hydrazono)-2-(3,4,5-trimethoxyphenyl)oxazol-5(4H)-one* ***8*** [89]. Orange solid (3.50 g, 70.01% yield); mp 88-90 °C; reported 90-91 °C.

*4.1.6. General procedure for the synthesis of compounds* ***9a-e***. A mixture of **8** (0.01 mol, 3.85 g), the appropriate amino acid (0.012 mol), and anhydrous sodium acetate (0.75 g) were dissolved in glacial acetic acid (25 mL). The reaction mixture was stirred under reflux for 2 h, and was left to cool, and was diluted with ice water. The precipitate formed was filtered off, washed with water, and re-crystallized from aqueous methanol.

*4.1.6.1. 2-(1-(3-Methoxyphenyl)-5-(3,4,5-trimethoxyphenyl)-1H-1,2,4-triazole-3-carboxamido)acetic acid **9a***. Reaction of **8** with glycine yielded pale yellow powder (2.10 g, 47.50%); mp 177-8°C; IR ($cm^{-1}$): 3675-2595 (OH), 3302 (NH), 1701 (C=O), 1669 (C=O), 1589 (C=N); $^1$H NMR (400 MHz, DMSO-$d_6$) δ (ppm): 3.61 (s, 6H, 2 OC$\underline{H}_3$), 3.69 (s, 3H, OC$\underline{H}_3$), 3.78 (s, 3H, OC$\underline{H}_3$), 3.95 (d, 2H, *J* = 7.20 Hz, HN-C$\underline{H}_2$-CO), 6.81 (s, 2H, 2 Ar-H), 7.07 (t, 1H, *J* = 7.80 Hz, Ar-H), 7.16 (d, 2H, *J* = 7.80 Hz, 2 Ar-H), 7.48 (s, 1H, Ar-H), 8.87 (t, 1H, *J* = 7.20 Hz, NH), 12.66 (br s, 1H, OH); $^{13}$C NMR (100 MHz, DMSO-$d_6$) δ (ppm): 171.3, 162.3, 160.3, 159.3, 156.1, 154.8, 153.1, 139.6, 139.1, 130.8, 122.3, 118.8, 118.1, 116.1, 112.4, 106.8, 60.6, 56.4, 56.2, 56.1, 41.4; HRMS: m/z calculated for $C_{21}H_{22}N_4O_7[M-H]^+$: 441.14157, found: 441.14221.

*4.1.6.2. 3-(1-(3-Methoxyphenyl)-5-(3,4,5-trimethoxyphenyl)-1H-1,2,4-triazole-3-carboxamido)propionic acid **9b***. Reaction of **8** with β-alanine yielded yellowish white powder (2.25 g, 49.34%); mp 189-91°C; IR ($cm^{-1}$): 3640-2540 (OH), 3301 (NH), 1698 (C=O), 1669 (C=O), 1592 (C=N); $^1$H NMR (400 MHz, DMSO-$d_6$) δ (ppm): 2.54 (t, 2H, *J* = 6.80 Hz, C$\underline{H}_2$-CO), 3.48-3.53 (m, 2H, HN-C$\underline{H}_2$), 3.61 (s, 6H, 2 OC$\underline{H}_3$), 3.69 (s, 3H, OC$\underline{H}_3$), 3.77 (s, 3H, OC$\underline{H}_3$), 6.80 (s, 2H, 2 Ar-H), 7.05 (t, 1H, *J* = 7.80 Hz, Ar-H), 7.14 (d, 2H, *J* = 7.80 Hz, 2 Ar-H), 7.47 (s, 1H, Ar-H), 8.65 (t, 1H, *J* = 6.80 Hz, NH), 12.30 (br s, 1H, OH); $^{13}$C NMR (100 MHz, DMSO-$d_6$) δ (ppm): 173.3, 160.3, 159.0, 156.4, 154.7, 153.1, 139.6, 139.1, 130.8, 122.3, 118.8, 116.1, 112.4, 106.8, 60.6, 56.2, 56.1, 35.4, 34.1; HRMS: m/z calculated for $C_{22}H_{24}N_4O_7[M-H]^+$: 455.15722, found: 455.15796.

*4.1.6.3. 4-(1-(3-Methoxyphenyl)-5-(3,4,5-trimethoxyphenyl)-1H-1,2,4-triazole-3-carboxamido)butyric acid **9c***. Reaction of **8** with 4-aminobutyric acid yielded yellowish white powder (2.30 g, 48.93%); mp 198-200°C; IR ($cm^{-1}$): 3640-2550 (OH), 3303 (NH), 1700 (C=O), 1667 (C=O), 1588 (C=N); $^1$H NMR (400 MHz, DMSO-$d_6$) δ (ppm): 1.77-1.83 (m, 2H, C$\underline{H}_2$-$CH_2$-CO), 2.55 (t, 2H, *J* = 6.80 Hz, C$\underline{H}_2$-CO), 3.55-3.58 (m, 2H, HN-C$\underline{H}_2$), 3.62 (s, 6H, 2 OC$\underline{H}_3$), 3.69 (s, 3H, OC$\underline{H}_3$), 3.79 (s, 3H, OC$\underline{H}_3$), 6.83 (s, 2H, 2 Ar-H), 7.05 (t, 1H, *J* = 8.00 Hz, Ar-H), 7.16 (d, 2H, *J* = 8.00 Hz, 2 Ar-H), 7.47 (s, 1H, Ar-H), 8.63 (t, 1H, *J* = 6.80 Hz, NH), 12.39 (br s, 1H, OH); $^{13}$C NMR (100 MHz, DMSO-$d_6$)

δ (ppm): 174.7, 160.3, 159.2, 156.6, 154.6, 153.1, 139.5, 139.2, 130.8, 122.4, 118.8, 116.1, 112.4, 106.8, 60.6, 56.2, 56.1, 38.6, 31.6, 25.0; HRMS: m/z calculated for $C_{23}H_{26}N_4O_7[M-H]^+$: 469.17287, found: 469.17322.

*4.1.6.4. 5-(1-(3-Methoxyphenyl)-5-(3,4,5-trimethoxyphenyl)-1H-1,2,4-triazole-3-carboxamido)pentanoic acid* ***9d***. Reaction of **8** with 5-aminovaleric acid yielded yellowish white powder (2.61 g, 53.73%); mp 211-3°C; IR ($cm^{-1}$): 3672-2569 (OH), 3299 (NH), 1701 (C=O), 1659 (C=O), 1594 (C=N); $^1$H NMR (400 MHz, DMSO-$d_6$) δ (ppm): 1.54-1.59 (m, 4H, C$\underline{H_2}$-C$\underline{H_2}$-CH$_2$-CO), 2.34 (t, 2H, *J* = 6.80 Hz, C$\underline{H_2}$-CO), 3.48-3.52 (m, 2H, HN-C$\underline{H_2}$), 3.61 (s, 6H, 2 OC$\underline{H_3}$), 3.69 (s, 3H, OC$\underline{H_3}$), 3.77 (s, 3H, OC$\underline{H_3}$), 6.80 (s, 2H, 2 Ar-H), 7.05 (t, 1H, *J* = 7.20 Hz, Ar-H), 7.15 (d, 2H, *J* = 7.20 Hz, 2 Ar-H), 7.47 (s, 1H, Ar-H), 8.66 (t, 1H, *J* = 6.80 Hz, NH), 12.44 (br s, 1H, OH); $^{13}$C NMR (100 MHz, DMSO-$d_6$) δ (ppm): 174.8, 162.3, 160.3, 159.0, 156.6, 154.6, 153.1, 139.5, 139.2, 130.8, 122.4, 118.8, 116.0, 112.4, 106.9, 60.6, 56.2, 56.1, 38.7, 33.8, 29.0, 22.3; HRMS: m/z calculated for $C_{24}H_{28}N_4O_7[M-H]^+$: 483.19157, found: 483.19215.

*4.1.6.5. 6-(1-(3-Methoxyphenyl)-5-(3,4,5-trimethoxyphenyl)-1H-1,2,4-triazole-3-carboxamido)hexanoic acid* ***9e***. Reaction of **8** with 6-aminohexanoic acid yielded pale yellow powder (2.35 g, 47.20%); mp 223-5°C; IR ($cm^{-1}$): 3629-2570 (OH), 3303 (NH), 1700 (C=O), 1666 (C=O), 1598 (C=N); $^1$H NMR (400 MHz, DMSO-$d_6$) δ (ppm): 1.23-1.26 (m, 2H, C$\underline{H_2}$-CH$_2$-CH$_2$-CO), 1.54-1.62 (m, 4H, C$\underline{H_2}$-CH$_2$-C$\underline{H_2}$-CH$_2$-CO), 2.58 (t, 2H, *J* = 6.20 Hz, C$\underline{H_2}$-CO), 3.56-3.58 (m, 2H, HN-C$\underline{H_2}$), 3.61 (s, 6H, 2 OC$\underline{H_3}$), 3.69 (s, 3H, OC$\underline{H_3}$), 3.78 (s, 3H, OC$\underline{H_3}$), 6.81 (s, 2H, 2 Ar-H), 7.07 (t, 1H, *J* = 8.00 Hz, Ar-H), 7.16 (d, 2H, *J* = 8.00 Hz, 2 Ar-H), 7.48 (s, 1H, Ar-H), 8.87 (t, 1H, *J* = 6.40 Hz, NH), 12.51 (br s, 1H, OH); $^{13}$C NMR (100 MHz, DMSO-$d_6$) δ (ppm): 174.9, 162.3, 160.3, 159.0, 156.6, 154.6, 153.1, 139.5, 139.2, 130.8, 128.6, 122.4, 116.0, 112.4, 111.9, 106.8, 60.6, 56.3, 56.2, 56.1, 38.5, 34.0, 29.3, 26.4, 24.7; HRMS: m/z calculated for $C_{25}H_{30}N_4O_7[M-H]^+$: 497.20417, found: 497.20513.

*4.1.7. General procedure for the synthesis of compounds* ***10a-e***. The acid **9** (0.01 mol) was dissolved in tetrahydrofuran (THF, 10 mL), *N*,*N*′-carbonyldiimidazole (CDI) (0.04 mol, 6.48 g) was

added at 25-30°C and stirred for 1 h. Hydroxylamine hydrochloride (0.04 mol, 2.78 g) was added, and the stirring was continued for another 1 h. The solvent was distilled off, ethylacetate (10 mL) was added, washed with water (2 x 10 mL), and the organic layer was collected, dried over anhydrous sodium sulphate, filtered, and evaporated under vacuum. The product was collected as oily droplets.

*4.1.7.1. 2-(1-(3-Methoxyphenyl)-5-(3,4,5-trimethoxyphenyl)-1H-1,2,4-triazole-3-carboxamido)-N-hydroxylacetamide* ***10a***. Pale brown oil (2.24 g, 49.01% yield); IR ($cm^{-1}$): 3402 (OH), 3365 (NH), 3302 (NH), 1707 (C=O), 1697 (C=O), 1589 (C=N); $^{1}$H NMR (400 MHz, DMSO-$d_6$) δ (ppm): 3.61 (s, 6H, 2 OC$\underline{H}_3$), 3.69 (s, 3H, OC$\underline{H}_3$), 3.78 (s, 3H, OC$\underline{H}_3$), 3.95 (d, 2H, *J* = 7.20 Hz, HN-C$\underline{H}_2$-CO), 6.81 (s, 2H, 2 Ar-H), 7.07 (t, 1H, *J* = 8.00 Hz, Ar-H), 7.16 (d, 2H, *J* = 8.00 Hz, 2 Ar-H), 7.48 (s, 1H, Ar-H), 8.87 (t, 1H, *J* = 7.20 Hz, NH), 11.51 (br s, 2H, NHOH); $^{13}$C NMR (100 MHz, DMSO-$d_6$) δ (ppm): 169.3, 162.3, 160.3, 159.2, 156.1, 154.8, 153.1, 139.6, 139.2, 130.8, 122.4, 118.8, 118.1, 116.1, 112.4, 106.8, 60.6, 56.4, 56.2, 56.1, 41.4; HRMS: m/z calculated for $C_{21}H_{23}N_5O_7[M-H]^+$: 456.15247, found: 456.15311.

*4.1.7.2. 3-(1-(3-Methoxyphenyl)-5-(3,4,5-trimethoxyphenyl)-1H-1,2,4-triazole-3-carboxamido)-N-hydroxypropionamide* ***10b***. Pale brown oil (2.31 g, 49.04% yield); IR ν ($cm^{-1}$): 3404 (OH), 3366 (NH), 3302 (NH), 1706 (C=O), 1698 (C=O), 1592 (C=N); $^{1}$H NMR (400 MHz, DMSO-$d_6$) δ (ppm): 2.53 (t, 2H, *J* = 6.80 Hz, C$\underline{H}_2$-CO), 3.51-3.56 (m, 2H, HN-C$\underline{H}_2$), 3.61 (s, 6H, 2 OC$\underline{H}_3$), 3.69 (s, 3H, OC$\underline{H}_3$), 3.78 (s, 3H, OC$\underline{H}_3$), 6.80 (s, 2H, 2 Ar-H), 7.05 (t, *J* = 8.00 Hz, 1H, Ar-H), 7.14 (d, 2H, *J* = 8.00 Hz, 2 Ar-H), 7.47 (s, 1H, Ar-H), 8.66 (t, 1H, *J* = 6.80 Hz, NH), 11.46 (br s, 2H, NHOH); $^{13}$C NMR (100 MHz, DMSO-$d_6$) δ (ppm): 169.6, 160.3, 159.0, 156.4, 154.7, 153.1, 139.6, 139.1, 130.8, 122.3, 118.8, 116.1, 112.4, 106.8, 60.6, 56.2, 56.1, 35.4, 34.1; HRMS: m/z calculated for $C_{22}H_{25}N_5O_7[M-H]^+$: 470.18124, found: 470.18213.

*4.1.7.3. 4-(1-(3-Methoxyphenyl)-5-(3,4,5-trimethoxyphenyl)-1H-1,2,4-triazole-3-carboxamido)-N-hydroxybutyramide* ***10c***. Brown oil (2.42 g, 49.89% yield); IR ν ($cm^{-1}$): 3402 (OH), 3366 (NH), 3301 (NH), 1705 (C=O), 1699 (C=O), 1588 (C=N); $^{1}$H NMR (400 MHz, DMSO-$d_6$) δ (ppm): 1.77-1.83 (m, 2H, C$\underline{H}_2$-$CH_2$-CO), 2.55 (t, 2H, *J* = 6.80 Hz, C$\underline{H}_2$-CO), 3.55-3.58 (m, 2H, HN-C$\underline{H}_2$), 3.62 (s, 6H, 2

OC$\underline{H}_3$), 3.69 (s, 3H, OC$\underline{H}_3$), 3.79 (s, 3H, OC$\underline{H}_3$), 6.83 (s, 2H, 2 Ar-H), 7.05 (t, 1H, *J* = 8.00 Hz, Ar-H), 7.16 (d, 2H, *J* = 8.00 Hz, 2 Ar-H), 7.47 (s, 1H, Ar-H), 8.63 (t, 1H, *J* = 6.80 Hz, NH), 11.30 (br s, 2H, NHOH); $^{13}$C NMR (100 MHz, DMSO-$d_6$) δ (ppm): 169.3, 162.3, 160.3, 159.2, 156.6, 154.6, 153.1, 139.6, 139.2, 130.8, 122.4, 118.8, 116.1, 112.4, 106.8, 60.6, 56.2, 56.1, 38.6, 30.6, 24.8; HRMS: m/z calculated for $C_{23}H_{27}N_5O_7[M-H]^+$: 484.19117, found: 484.19194.

*4.1.7.4. 5-(1-(3-Methoxyphenyl)-5-(3,4,5-trimethoxyphenyl)-1H-1,2,4-triazole-3-carboxamido)-N-hydroxypentanamide* ***10d***. Brown oil (2.61 g, 52.3% yield); IR ν (cm$^{-1}$): 3402 (OH), 3365 (NH), 3302 (NH), 1707 (C=O), 1697 (C=O), 1594 (C=N); $^1$H NMR (400 MHz, DMSO-$d_6$) δ (ppm): 1.54-1.59 (m, 4H, C$\underline{H}_2$-C$\underline{H}_2$-CH$_2$-CO), 2.34 (t, 2H, *J* = 6.80 Hz, C$\underline{H}_2$-CO), 3.48-3.52 (m, 2H, HN-C$\underline{H2}$), 3.61 (s, 6H, 2 OC$\underline{H}_3$), 3.69 (s, 3H, OC$\underline{H}_3$), 3.77 (s, 3H, OC$\underline{H}_3$), 6.80 (s, 2H, 2 Ar-H), 7.05 (t, 1H, *J* = 8.00 Hz, Ar-H), 7.15 (d, 2H, *J* = 8.00 Hz, 2 Ar-H), 7.47 (s, 1H, Ar-H), 8.65 (t, 1H, *J* = 6.80 Hz, NH), 11.22 (br s, 2H, NHOH); $^{13}$C NMR (100 MHz, DMSO-$d_6$) δ (ppm): 167.0, 162.3, 160.3, 159.0, 156.6, 154.6, 153.1, 139.5, 139.2, 130.8, 122.4, 118.8, 116.0, 112.4, 106.9, 60.6, 56.2, 56.1, 38.7, 32.8, 29.0, 22.3; HRMS: m/z calculated for $C_{24}H_{29}N_5O_7[M-H]^+$: 498.19882, found: 498.19916.

*4.1.7.5. 6-(1-(3-Methoxyphenyl)-5-(3,4,5-trimethoxyphenyl)-1H-1,2,4-triazole-3-carboxamido)-N-hydroxyhexanamide* ***10e***. Pale brown oil (2.57 g, 50.09% yield); IR (cm$^{-1}$): 3405 (OH), 3365 (NH), 3306 (NH), 1707 (C=O), 1699 (C=O), 1598 (C=N); $^1$H NMR (400 MHz, DMSO-$d_6$) δ (ppm): 1.23-1.26 (m, 2H, C$\underline{H}_2$-CH$_2$-CH$_2$-CO), 1.54-1.62 (m, 4H, C$\underline{H}_2$-CH$_2$-C$\underline{H}_2$-CH$_2$-CO), 2.58 (t, 2H, *J* = 6.20 Hz, C$\underline{H}_2$-CO), 3.56-3.58 (m, 2H, HN-C$\underline{H}_2$), 3.61 (s, 6H, 2 OC$\underline{H}_3$), 3.69 (s, 3H, OC$\underline{H}_3$), 3.78 (s, 3H, OC$\underline{H}_3$), 6.81 (s, 2H, 2 Ar-H), 7.07 (t, 1H, *J* = 8.00 Hz, Ar-H), 7.16 (d, 2H, *J* = 8.00 Hz, 2 Ar-H), 7.48 (s, 1H, Ar-H), 8.86 (t, 1H, *J* = 6.80 Hz, NH), 11.32 (br s, 2H, NHOH); $^{13}$C NMR (100 MHz, DMSO-$d_6$) δ (ppm): 169.6, 162.3, 160.3, 159.0, 156.6, 154.6, 153.1, 139.6, 139.2, 130.8, 128.6, 122.4, 116.0, 112.4, 106.8, 60.6, 56.3, 56.2, 56.1, 38.5, 33.3, 29.3, 26.4, 24.3; HRMS: m/z calculated for $C_{25}H_{31}N_5O_7[M-H]^+$: 512.21507, found: 512.21304.

*4.2. Biological evaluation*

*4.2.1. In vitro anti-proliferative activity assay*

Cancer cells from different cancer cell lines; human breast adenocarcinoma (MCF7) and human hepatocellular carcinoma (HepG2) were purchased from American type Cell Culture collection (ATCC, Manassas, USA) and grown on Dulbecco's modified Eagle's medium (DMEM) or Roswell Park Memorial Institute medium (RPMI 1640) supplemented with 100 mg/ mL of streptomycin, 100 units/ mL of penicillin, and 10% of heat-inactivated fetal bovine serum. The cell lines were kept in a humidified, 5% (v/v) $CO_2$ atmosphere at 37 ºC. Exponentially growing cells from the two cancer cell lines were trypsinized (for detachment), counted and seeded at the appropriate densities (2000-1000 cells/0.33 $cm^2$ well) into 96-well microtiter plates. Cells then were incubated in a humidified atmosphere at 37˚C for 24 hours. Then, cells were exposed to different concentrations of compounds 4a-f, 5a-f, 9a-e, 10a-e, SAHA, and CA4 (0.1,1, 10,100,1000 µM) for 72 h. The viability of treated cells was determined using MTT technique. Media were removed, cells were incubated with MTT (5%, 200 µL) solution/well (Sigma Aldrich, MO, USA), and were allowed to metabolize the dye into a colored-insoluble formazan crystals for 2 h. The remaining MTT solution were discarded from the wells and the formazan crystals were dissolved in 200 µL/well acidified isopropanol for 30 min, covered with aluminum foil and continuously shaken using a MaxQ 2000 plate shaker (Thermo Fisher Scientific Inc, MI, USA) at room temperature. Absorbances were measured at 570 nm using a Stat Fax$^R$ 4200 plate reader (Awareness Technology, Inc., FL, USA). The cell viability were expressed as percentage of control and the concentration that induces 50% of maximum inhibition of cell proliferation ($IC_{50}$) were determined using Graph Pad Prism 5 software (Graph Pad software Inc, CA) [90, 91].

*4.2.2. In vitro enzyme inhibitory assays*

HeLa cells and MCF-7 cell lines were obtained from American Type Culture Collection, cells were cultured using Dulbecco's Modified Eagle's Medium (DMEM) (Invitrogen/Life Technologies) supplemented with 10% Fetal Bovine Serum (FBS) (Hyclone,), 10 µg/mL of insulin (Sigma), and 1% penicillin-streptomycin. All of the other chemicals and reagents were from Sigma, or Invitrogen. Cells

were plated (cells density 1.2 – 1.8 × 100,000 cells/well) in a volume of 100 µL complete growth medium + 100 µL of the tested compound per well in a 96-well plate for 18-24 h before the enzyme assay for HDAC and Tubulin.

*4.2.2.1. HDAC inhibitory assay*

The *in vitro* HDAC inhibitory activities of compounds **5f, 10a** and **10e** against four HDAC isoforms (HDAC1, 2, 4, 6) were measured using ELISA assay kits (Mybiosource, Inc.) according to manufacturer's directions. Briefly, HeLa cells were trypsinized, counted and seeded at the appropriate densities into 96-well microtiter plates. Cells then were incubated in a humidified atmosphere at 37˚C for 24 h. The standards, the tested compounds, and the positive reference SAHA were diluted to designated concentrations. On the 96-well microtiter plates standard or sample was added to each well in 100 µL, and incubated at 37 °C for 2 h. The solution was aspirated and 100 µL of prepared Detection Reagent A was added to each well. Incubation was done at 37°C for 2 h. After washing 100 µL of prepared Detection Reagent B was added and incubation was continued at 37°C for 30 min. Five washings were done, then 90 µL of 3,3',5,5'-tetramethylbenzidine (TMB) substrate solution was added and incubated at 37°C for 15-25 min. Stop solution was added in 50 µL. Cells were exposed to different concentrations of compounds **5f**, **10a**, **10e** and SAHA (0.01,0.1, 1,10 µM) for 72 h. Optical density (O.D.) was measured at 450 nm using microplate reader (Spectromax Plus 96 well plate spectrophotometer), and the concentration that induces 50% of maximum inhibition of HDAC isoforms ($IC_{50}$) were determined using Graph Pad Prism 5 software (Graph Pad software Inc, CA).

*4.2.2.2. Tubulin polymerization inhibitory assay*

*In vitro* kinetics of microtubule assembly were measured using ELISA kit for TUBb (Cloud-Clone. Corp.) on MCF-7 cell line. The compounds tested were **9a**, **10a**, **10e**, and CA4. Briefly, growing cells from MCF-7 cell lines were trypsinized, counted and seeded at the appropriate densities into 96-well microtiter plates. Cells then were incubated in a humidified atmosphere at 37˚C for 24 h. The standards, the tested compounds, and the control CA4 were diluted to designated concentrations. On the 96-well

microtiter plates standard or sample was added to each well in 100 µL, and incubated at 37°C for 2 h. The solution was aspirated and 100 µL of prepared Detection Reagent A was added to each well. Incubation was done at 37°C for 2 h. After washing 100 µL of prepared Detection Reagent B was added and incubation was continued at 37°C for 30 min. Five washings were done, then 90 µL of 3,3',5,5'-tetramethylbenzidine (TMB) substrate solution was added and incubated at 37°C for 15-25 min. Stop solution was added in 50 µL. Cells were exposed to different concentrations of compounds **9a**, **10a**, **10e** and CA4 (0.4,2, 10,50 µM) for 72 h. Optical density (O.D.) was measured at 450 nm using microplate reader (Spectromax Plus 96 well plate spectrophotometer), and the concentration that induces 50% of maximum inhibition of TUBb ($IC_{50}$) were determined using Graph Pad Prism 5 software (Graph Pad software Inc, CA) [90, 91].

*Docking studies*

Discovery Studio 2.5 software (Accelrys Inc., San Diego, CA, USA) was used for docking analysis. Fully automated docking tool using "Dock ligands (CDocker)" protocol running on Intel(R) core(TM) i32370 CPU @ 2.4 GHz 2.4 GHz, RAM Memory 2 GB under the Windows 7.0 system. The receptor protein is prepared. The force field applied is CharmM to the receptor and the hydrogens are minimized. By selecting only the ligand part and clicking on "Define sphere from selection" so that the crystal ligand is used to define the binding site of 13, 11 Angstroms for tubulin and HDAC, respectively, on the receptor molecule. Now the above prepared receptor is given as input for "input receptor molecule" parameter in the CDocker protocol parameter explorer. Force fields are applied on compounds **5f**, **5e**, **9a**, **10a** and **10e** to get the minimum lowest energy structure. The obtained poses were studied and the poses showing best ligand–tubulin or HDAC interactions were selected and used for CDocker energy (protein-ligand interaction energies) calculations.

*4.2.2.3. Docking of the target molecules to HDLP in vorinostat binding site.*

Compounds **5f**, **5e**, **10a**, **10e** and vorinostat were docked into the empty vorinostat binding site of HDLP (Histone Deacetylase Like Protein) a homologue from hyperthermophilic bacterium Aquifex aeolicus,

that shares 35.2% identity with human HDAC 1 over 375 residues. Docking of the conformation database of the target compound was done using Discovery Studio 2.5 software program. The X-ray crystallographic structure of HDLP complexed with vorinostat was obtained from the Protein Data Bank (http://www. rcsb.org/, PDB code 1C3S) [36].

*4.2.2.4. Docking of the target molecules to tubulin protein in the colchicine binding site*

Compounds **9a**, **10a**, **10e** and CA4 were docked into the empty colchicine binding site of tubulin. Docking of the conformation database of the target compound was done using Discovery Studio 2.5 software program. The X-ray crystallographic structure of tubulin complexed with DAMA-colchicine was obtained from the Protein Data Bank (http://www. rcsb.org/, PDB code 1SA0) [85].

*Acknowledgments*

The authors are thankful to Dr. Tamer Abdelghany, Faculty of Pharmacy, Al-Azhar University, Cairo, for performing the anti-proliferative activity of the compounds. The help rendered by Dr. Esam Rashwan, at Serum and Vaccine Research Institute, for performing the tubulin and HDAC inhibitory activity assays is gratefully acknowledged.

## 5. *References*

1. Yoo, C. B.; Jones, P. A. Epigenetic Therapy of Cancer: Past, Present and Future. *Nat. rev.Drug discov.* **2006,** *5*, 37-50.

2. Jiao, P.-F.; Zhao, B.-X.; Wang, W.-W.; He, Q.-X.; Wan, M.-S.; Shin, D.-S.; Miao, J.-Y. Design, Synthesis, and Preliminary Biological Evaluation of 2, 3-Dihydro-3-Hydroxymethyl-1, 4-Benzoxazine Derivatives. *Bioorg. Med. Chem. Lett.* **2006,** *16*, 2862-2867.

3. Toyota, M.; Issa, J.-P. J. In *Epigenetic Changes in Solid and Hematopoietic Tumors*, Semin. Oncol., 2005; Elsevier: 2005; pp 521-530.

4. Wade, P. A. Transcriptional Control at Regulatory Checkpoints by Histone Deacetylases: Molecular Connections between Cancer and Chromatin. *Hum. Mol. Genet.* **2001,** *10*, 693-698.

5. Jenuwein, T.; Allis, C. D. Translating the Histone Code. *Science* **2001,** *293*, 1074-1080.

6. Witt, O.; Deubzer, H. E.; Milde, T.; Oehme, I. Hdac Family: What Are the Cancer Relevant Targets? *Cancer Lett.* **2009,** *277*, 8-21.

7. Turner, B. M. Cellular Memory and the Histone Code. *Cell* **2002,** *111*, 285-291.

8. Bolden, J. E.; Peart, M. J.; Johnstone, R. W. Anticancer Activities of Histone Deacetylase Inhibitors. *Nat. rev. Drug discov.* **2006,** *5*, 769-784.

9. De Ruijter, A.; Van Gennip, A.; Caron, H.; Kemp, S.; Van Kuilenburg, A. Histone Deacetylases (Hdacs): Characterization of the Classical Hdac Family. *Biochem. J* **2003,** *370*, 737-749.

10. Minucci, S.; Pelicci, P. G. Histone Deacetylase Inhibitors and the Promise of Epigenetic (and More) Treatments for Cancer. *Nat. rev. Cancer* **2006,** *6*, 38-51.

11. Haberland, M.; Montgomery, R. L.; Olson, E. N. The Many Roles of Histone Deacetylases in Development and Physiology: Implications for Disease and Therapy. *Nat. rev. Genetics* **2009,** *10*, 32-42.

12. Glozak, M. A.; Sengupta, N.; Zhang, X.; Seto, E. Acetylation and Deacetylation of Non-Histone Proteins. *Gene* **2005,** *363*, 15-23.

13. Fass, D. M.; Kemp, M. M.; Schroeder, F. A.; Wagner, F. F.; Wang, Q.; Holson, E. B. Histone Acetylation and Deacetylation. *Encyclopedia of Molecular Cell Biology and Molecular Medicine* **2012**.

14. West, A. C.; Johnstone, R. W. New and Emerging Hdac Inhibitors for Cancer Treatment. *J. clin. investig.* **2014,** *124*, 30-39.

15. Kazantsev, A. G.; Thompson, L. M. Therapeutic Application of Histone Deacetylase Inhibitors for Central Nervous System Disorders. *Nat. rev. Drug discov.* **2008,** *7*, 854-868.

16. Archin, N. M.; Liberty, A.; Kashuba, A. D.; Choudhary, S. K.; Kuruc, J.; Crooks, A.; Parker, D.; Anderson, E.; Kearney, M.; Strain, M. Erratum: Administration of Vorinostat Disrupts Hiv-1 Latency in Patients on Antiretroviral Therapy. *Nature* **2012,** *489*, 460-460.

17. Royce, S. G.; Karagiannis, T. C. Histone Deacetylases and Their Inhibitors: New Implications for Asthma and Chronic Respiratory Conditions. *Curr. Opin. Allergy Clin. Immunol.* **2014,** *14*, 44-48.

18. Weichert, W. Hdac Expression and Clinical Prognosis in Human Malignancies. *Cancer Lett.* **2009,** *280*, 168-176.

19. Gregoretti, I.; Lee, Y.-M.; Goodson, H. V. Molecular Evolution of the Histone Deacetylase Family: Functional Implications of Phylogenetic Analysis. *J. Mol. Biol.* **2004,** *338*, 17-31.

20. Batty, N.; Malouf, G. G.; Issa, J. P. J. Histone Deacetylase Inhibitors as Anti-Neoplastic Agents. *Cancer Lett.* **2009,** *280*, 192-200.

21. Marks, P. A.; Rifkind, R. A.; Richon, V. M.; Breslow, R.; Miller, T.; Kelly, W. K. Histone Deacetylases and Cancer: Causes and Therapies. *Nat. rev. Cancer* **2001,** *1*, 194-202.

22. Li, J.; Li, G.; Xu, W. Histone Deacetylase Inhibitors: An Attractive Strategy for Cancer Therapy. *Curr. Med. Chem.* **2013,** *20*, 1858-1886.

23. Dokmanovic, M.; Clarke, C.; Marks, P. A. Histone Deacetylase Inhibitors: Overview and Perspectives. *Mol. Cancer Res.* **2007,** *5*, 981-989.

24. Saito, A.; Yamashita, T.; Mariko, Y.; Nosaka, Y.; Tsuchiya, K.; Ando, T.; Suzuki, T.; Tsuruo, T.; Nakanishi, O. A Synthetic Inhibitor of Histone Deacetylase, Ms-27-275, with Marked in Vivo Antitumor Activity against Human Tumors. *Proc. Natl. Acad. Sci. U. S. A.* **1999,** *96*, 4592-4597.

25. Glick, R. D.; Swendeman, S. L.; Coffey, D. C.; Rifkind, R. A.; Marks, P. A.; Richon, V. M.; La Quaglia, M. P. Hybrid Polar Histone Deacetylase Inhibitor Induces Apoptosis and Cd95/Cd95 Ligand Expression in Human Neuroblastoma. *Cancer Res.* **1999,** *59*, 4392-4399.

26. Butler, L. M.; Agus, D. B.; Scher, H. I.; Higgins, B.; Rose, A.; Cordon-Cardo, C.; Thaler, H. T.; Rifkind, R. A.; Marks, P. A.; Richon, V. M. Suberoylanilide Hydroxamic Acid, an Inhibitor of Histone Deacetylase, Suppresses the Growth of Prostate Cancer Cells in Vitro and in Vivo. *Cancer Res.* **2000,** *60*, 5165-5170.

27. Oyelere, A. K.; Chen, P. C.; Guerrant, W.; Mwakwari, S. C.; Hood, R.; Zhang, Y.; Fan, Y. Non-Peptide Macrocyclic Histone Deacetylase Inhibitors. *J. Med. Chem.* **2008,** *52*, 456-468.

28. Grant, S.; Easley, C.; Kirkpatrick, P. Vorinostat. *Nat. rev. Drug discov.* **2007,** *6*, 21-22.

29. Mann, B. S.; Johnson, J. R.; Cohen, M. H.; Justice, R.; Pazdur, R. Fda Approval Summary: Vorinostat for Treatment of Advanced Primary Cutaneous T-Cell Lymphoma. *The oncologist* **2007,** *12*, 1247-1252.

30. Chien, W.; Lee, D. H.; Zheng, Y.; Wuensche, P.; Alvarez, R.; Wen, D. L.; Aribi, A. M.; Thean, S. M.; Doan, N. B.; Said, J. W. Growth Inhibition of Pancreatic Cancer Cells by Histone Deacetylase Inhibitor Belinostat through Suppression of Multiple Pathways Including Hif, Nfkb, and Mtor Signaling in Vitro and in Vivo. *Mol. Carcinog.* **2014,** *53*, 722-735.

31. Grant, C.; Rahman, F.; Piekarz, R.; Peer, C.; Frye, R.; Robey, R. W.; Gardner, E. R.; Figg, W. D.; Bates, S. E. Romidepsin: A New Therapy for Cutaneous T-Cell Lymphoma and a Potential Therapy for Solid Tumors. **2010**.

32. Mwakwari, S. C.; Patil, V.; Guerrant, W.; Oyelere, A. K. Macrocyclic Histone Deacetylase Inhibitors. *Curr. Top. Med. Chem.* **2010,** *10*, 1423.

33. Rajkumar, S. V. Panobinostat for the Treatment of Multiple Myeloma. *Lancet Oncol.* **2014,** *15*, 1178.

34. Paris, M.; Porcelloni, M.; Binaschi, M.; Fattori, D. Histone Deacetylase Inhibitors: From Bench to Clinic. *J. Med. Chem.* **2008,** *51*, 1505-1529.

35. Arrowsmith, C. H.; Bountra, C.; Fish, P. V.; Lee, K.; Schapira, M. Epigenetic Protein Families: A New Frontier for Drug Discovery. *Nat. rev. Drug discov.* **2012,** *11*, 384-400.

36. Finnin, M. S.; Donigian, J. R.; Cohen, A.; Richon, V. M.; Rifkind, R. A.; Marks, P. A.; Breslow, R.; Pavletich, N. P. Structures of a Histone Deacetylase Homologue Bound to the Tsa and Saha Inhibitors. *Nature* **1999,** *401*, 188-193.

37. Vannini, A.; Volpari, C.; Filocamo, G.; Casavola, E. C.; Brunetti, M.; Renzoni, D.; Chakravarty, P.; Paolini, C.; De Francesco, R.; Gallinari, P. Crystal Structure of a Eukaryotic Zinc-Dependent Histone Deacetylase, Human Hdac8, Complexed with a Hydroxamic Acid Inhibitor. *Proc. Natl. Acad. Sci. U. S. A.* **2004,** *101*, 15064-15069.

38. Somoza, J. R.; Skene, R. J.; Katz, B. A.; Mol, C.; Ho, J. D.; Jennings, A. J.; Luong, C.; Arvai, A.; Buggy, J. J.; Chi, E. Structural Snapshots of Human Hdac8 Provide Insights into the Class I Histone Deacetylases. *Structure* **2004,** *12*, 1325-1334.

39. Bottomley, M. J.; Surdo, P. L.; Di Giovine, P.; Cirillo, A.; Scarpelli, R.; Ferrigno, F.; Jones, P.; Neddermann, P.; De Francesco, R.; Steinkühler, C. Structural and Functional Analysis of the Human Hdac4 Catalytic Domain Reveals a Regulatory Structural Zinc-Binding Domain. *J. Biol. Chem.* **2008,** *283*, 26694-26704.

40. Watson, P. J.; Fairall, L.; Santos, G. M.; Schwabe, J. W. Structure of Hdac3 Bound to Co-Repressor and Inositol Tetraphosphate. *Nature* **2012,** *481*, 335-340.

41. Bressi, J. C.; Jennings, A. J.; Skene, R.; Wu, Y.; Melkus, R.; De Jong, R.; O'connell, S.; Grimshaw, C. E.; Navre, M.; Gangloff, A. R. Exploration of the Hdac2 Foot Pocket: Synthesis and Sar of Substituted N-(2-Aminophenyl) Benzamides. *Bioorg. Med. Chem. Lett.* **2010,** *20*, 3142-3145.

42. Sternson, S. M.; Wong, J. C.; Grozinger, C. M.; Schreiber, S. L. Synthesis of 7200 Small Molecules Based on a Substructural Analysis of the Histone Deacetylase Inhibitors Trichostatin and Trapoxin. *Org. Lett.* **2001,** *3*, 4239-4242.

43. Oanh, D. T. K.; Van Hai, H.; Park, S. H.; Kim, H.-J.; Han, B.-W.; Kim, H.-S.; Hong, J.-T.; Han, S.-B.; Nam, N.-H. Benzothiazole-Containing Hydroxamic Acids as Histone Deacetylase Inhibitors and Antitumor Agents. *Bioorg. Med. Chem. Lett.* **2011,** *21*, 7509-7512.

44. Zhang, X.; Zhang, J.; Tong, L.; Luo, Y.; Su, M.; Zang, Y.; Li, J.; Lu, W.; Chen, Y. The Discovery of Colchicine-Saha Hybrids as a New Class of Antitumor Agents. *Biorg. Med. Chem.* **2013,** *21*, 3240-3244.

45. Guan, P.; Sun, F. E.; Hou, X.; Wang, F.; Yi, F.; Xu, W.; Fang, H. Design, Synthesis and Preliminary Bioactivity Studies of 1, 3, 4-Thiadiazole Hydroxamic Acid Derivatives as Novel Histone Deacetylase Inhibitors. *Biorg. Med. Chem*. **2012,** *20*, 3865-3872.

46. Guandalini, L.; Balliu, M.; Cellai, C.; Martino, M.; Nebbioso, A.; Mercurio, C.; Carafa, V.; Bartolucci, G.; Dei, S.; Manetti, D. Design, Synthesis and Preliminary Evaluation of a Series of Histone Deacetylase Inhibitors Carrying a Benzodiazepine Ring. *Eur. J. Med. Chem.* **2013,** *66*, 56-68.

47. Abdel-Aziz, M.; A Metwally, K.; Gamal-Eldeen, A. M.; M Aly, O. 1, 3, 4-Oxadiazole-2-Thione Derivatives; Novel Approach for Anticancer and Tubulin Polymerization Inhibitory Activities. *Anti-Cancer Agents in Medicinal Chemistry (Formerly Current Medicinal Chemistry-Anti-Cancer Agents)* **2016,** *16*, 269-277.

48. Aly, O. M.; Beshr, E. A.; Maklad, R. M.; Mustafa, M.; Gamal-Eldeen, A. M. Synthesis, Cytotoxicity, Docking Study, and Tubulin Polymerization Inhibitory Activity of Novel 1-(3, 4-Dimethoxyphenyl)-5-(3, 4, 5-Trimethoxyphenyl)-1h-1, 2, 4-Triazole-3-Carboxanilides. *Arch. Pharm.* **2014,** *347*, 658-667.

49. Bhattacharyya, B.; Panda, D.; Gupta, S.; Banerjee, M. Anti-Mitotic Activity of Colchicine and the Structural Basis for Its Interaction with Tubulin. *Med. Res. Rev.* **2008,** *28*, 155-183.

50. Pettit, G. R.; Cragg, G. M.; Herald, D. L.; Schmidt, J. M.; Lohavanijaya, P. Isolation and Structure of Combretastatin. *Can. J. Chem.* **1982,** *60*, 1374-1376.

51. Pettit, G. R.; Cragg, G. M.; Singh, S. B. Antineoplastic Agents, 122. Constituents of Combretum Caffrum. *J. Nat. Prod.* **1987,** *50*, 386-391.

52. Pettit, G.; Singh, S.; Hamel, E.; Lin, C. M.; Alberts, D.; Garcia-Kendal, D. Isolation and Structure of the Strong Cell Growth and Tubulin Inhibitor Combretastatin a-4. *Experientia* **1989,** *45*, 209-211.

53. Mcgown, A. T.; Fox, B. W. Differential Cytotoxicity of Combretastatins A1 and A4 in Two Daunorubicin-Resistant P388 Cell Lines. *Cancer Chemother. Pharmacol.* **1990,** *26*, 79-81.

54. Pettit, G. R.; Rhodes, M. R.; Herald, D. L.; Hamel, E.; Schmidt, J. M.; Pettit, R. K. Antineoplastic Agents. 445. Synthesis and Evaluation of Structural Modifications of (Z)-and (E)-Combretastatin a-4 1. *J. Med. Chem.* **2005,** *48*, 4087-4099.

55. Dark, G. G.; Hill, S. A.; Prise, V. E.; Tozer, G. M.; Pettit, G. R.; Chaplin, D. J. Combretastatin a-4, an Agent That Displays Potent and Selective Toxicity toward Tumor Vasculature. *Cancer Res.* **1997,** *57*, 1829-1834.

56. Chaplin, D.; Dougherty, G. Tumour Vasculature as a Target for Cancer Therapy. *Br. J. Cancer* **1999,** *80*, 57-64.

57. Tozer, G. M.; Kanthou, C.; Parkins, C. S.; Hill, S. A. The Biology of the Combretastatins as Tumour Vascular Targeting Agents. *Int. J. Exp. Pathol.* **2002,** *83*, 21-38.

58. Pettit, G. R.; Rhodes, M.; Herald, D.; Chaplin, D.; Stratford, M.; Hamel, E.; Pettit, R.; Chapuis, J.; Oliva, D. Antineoplastic Agents 393. Synthesis of the Trans-Isomer of Combretastatin a-4 Prodrug. *Anti-Cancer Drug Des.* **1998,** *13*, 981-993.

59. Pettit, G. R.; Toki, B. E.; Herald, D. L.; Boyd, M. R.; Hamel, E.; Pettit, R. K.; Chapuis, J. C. Antineoplastic Agents. 410. Asymmetric Hydroxylation of Trans-Combretastatin a-4 1. *J. Med. Chem.* **1999,** *42*, 1459-1465.

60. Li, Y.; Luo, P.; Wang, J.; Dai, J.; Yang, X.; Wu, H.; Yang, B.; He, Q. Autophagy Blockade Sensitizes the Anticancer Activity of Ca-4 Via Jnk-Bcl-2 Pathway. *Toxicol. Appl. Pharmacol.* **2014,** *274*, 319-327.

61. Aprile, S.; Del Grosso, E.; Tron, G. C.; Grosa, G. In Vitro Metabolism Study of Combretastatin a-4 in Rat and Human Liver Microsomes. *Drug Metab. Disposition* **2007,** *35*, 2252-2261.

62. Siemann, D. W.; Chaplin, D. J.; Walicke, P. A. A Review and Update of the Current Status of the Vasculature-Disabling Agent Combretastatin-A4 Phosphate (Ca4p). *Expert opin. investig. drugs* **2009,** *18*, 189-197.

63. Dowlati, A.; Robertson, K.; Cooney, M.; Petros, W. P.; Stratford, M.; Jesberger, J.; Rafie, N.; Overmoyer, B.; Makkar, V.; Stambler, B. A Phase I Pharmacokinetic and Translational Study of the Novel Vascular Targeting Agent Combretastatin a-4 Phosphate on a Single-Dose Intravenous Schedule in Patients with Advanced Cancer. *Cancer Res.* **2002,** *62*, 3408-3416.

64. Cirla, A.; Mann, J. Combretastatins: From Natural Products to Drug Discovery. *Nat. Prod. Rep.* **2003,** *20*, 558-564.

65. Pinney, K. G.; Jelinek, C.; Edvardsen, K.; Chaplin, D.; Pettit, G. The Discovery and Development of the Combretastatins. *Anticancer agents from natural products* **2005**, 23-46.

66. Hsieh, H.; Liou, J.; Mahindroo, N. Pharmaceutical Design of Antimitotic Agents Based on Combretastatins. *Curr. Pharm. Des.* **2005,** *11*, 1655-1677.

67. Brown, T.; Holt Jr, H.; Lee, M. Synthesis of Biologically Active Heterocyclic Stilbene and Chalcone Analogs of Combretastatin. In *Heterocyclic Antitumor Antibiotics*, Springer: 2006; pp 1-51.

68. Tron, G. C.; Pirali, T.; Sorba, G.; Pagliai, F.; Busacca, S.; Genazzani, A. A. Medicinal Chemistry of Combretastatin A4: Present and Future Directions. *J. Med. Chem.* **2006,** *49*, 3033-3044.

69. Brancale, A.; Silvestri, R. Indole, a Core Nucleus for Potent Inhibitors of Tubulin Polymerization. *Med. Res. Rev.* **2007,** *27*, 209-238.

70. Shan, Y. S.; Zhang, J.; Liu, Z.; Wang, M.; Dong, Y. Developments of Combretastatin a-4 Derivatives as Anticancer Agents. *Curr. Med. Chem.* **2011,** *18*, 523-538.

71. Marrelli, M.; Conforti, F.; A Statti, G.; Cachet, X.; Michel, S.; Tillequin, F.; Menichini, F. Biological Potential and Structure-Activity Relationships of Most Recently Developed Vascular Disrupting Agents: An Overview of New Derivatives of Natural Combretastatin a-4. *Curr. Med. Chem.* **2011,** *18*, 3035-3081.

72. Singh, R.; Kaur, H. Advances in Synthetic Approachesfor the Preparation of Combretastatin-Based Anti-Canceragents. *Synthesis* **2009,** *2009*, 2471-2491.

73. Jordan, A.; Hadfield, J. A.; Lawrence, N. J.; Mcgown, A. T. Tubulin as a Target for Anticancer Drugs: Agents Which Interact with the Mitotic Spindle. *Med. Res. Rev.* **1998,** *18*, 259-296.

74. Chen, H.; Li, Y.; Sheng, C.; Lv, Z.; Dong, G.; Wang, T.; Liu, J.; Zhang, M.; Li, L.; Zhang, T. Design and Synthesis of Cyclopropylamide Analogues of Combretastatin-A4 as Novel Microtubule-Stabilizing Agents. *J. Med. Chem.* **2013,** *56*, 685-699.

75. Simoni, D.; Grisolia, G.; Giannini, G.; Roberti, M.; Rondanin, R.; Piccagli, L.; Baruchello, R.; Rossi, M.; Romagnoli, R.; Invidiata, F. P. Heterocyclic and Phenyl Double-Bond-Locked Combretastatin Analogues Possessing Potent Apoptosis-Inducing Activity in Hl60 and in Mdr Cell Lines. *J. Med. Chem.* **2005,** *48*, 723-736.

76. Romagnoli, R.; Baraldi, P. G.; Salvador, M. K.; Preti, D.; Aghazadeh Tabrizi, M.; Brancale, A.; Fu, X.-H.; Li, J.; Zhang, S.-Z.; Hamel, E. Discovery and Optimization of a Series of 2-Aryl-4-Amino-5-(3′, 4′, 5′-Trimethoxybenzoyl) Thiazoles as Novel Anticancer Agents. *J. Med. Chem.* **2012,** *55*, 5433-5445.

77. Li, J. J. Bucherer—Bergs Reaction. *Name Reactions* **2009**, 76-77.

78. Usachova, N.; Leitis, G.; Jirgensons, A.; Kalvinsh, I. Synthesis of Hydroxamic Acids by Activation of Carboxylic Acids with N,N′-Carbonyldiimidazole: Exploring the Efficiency of the Method. *Synth. Commun.* **2010,** *40*, 927-935.

79. Padiya, K. J.; Gavade, S.; Kardile, B.; Tiwari, M.; Bajare, S.; Mane, M.; Gaware, V.; Varghese, S.; Harel, D.; Kurhade, S. Unprecedented “in Water” Imidazole Carbonylation: Paradigm Shift for Preparation of Urea and Carbamate. *Org. Lett.* **2012,** *14*, 2814-2817.

80. Abdel-Aziz, M.; Beshr, E. A.; Abdel-Rahman, I. M.; Ozadali, K.; Tan, O. U.; Aly, O. M. 1-(4-Methoxyphenyl)-5-(3, 4, 5-Trimethoxyphenyl)-1h-1, 2, 4-Triazole-3-Carboxamides: Synthesis, Molecular Modeling, Evaluation of Their Anti-Inflammatory Activity and Ulcerogenicity. *Eur. J. Med. Chem.* **2014,** *77*, 155-165.

81. Sawdey, G. W. Rearrangement of 4-Arylazo-2-Phenyloxazolin-5-Ones: A New Synthesis of 1h-1, 2, 4-Triazoles. *J. Am. Chem. Soc.* **1957,** *79*, 1955-1956.

82. Koska, J. R.; Spassov, V. Z.; Maynard, A. J.; Yan, L.; Austin, N.; Flook, P. K.; Venkatachalam, C. Fully Automated Molecular Mechanics Based Induced Fit Protein− Ligand Docking Method. *J. Chem. Inf. Model.* **2008,** *48*, 1965-1973.

83. Wu, G.; Robertson, D. H.; Brooks, C. L., 3rd; Vieth, M. Detailed Analysis of Grid-Based Molecular Docking: A Case Study of Cdocker-a Charmm-Based Md Docking Algorithm. *J. Comput. Chem.* **2003,** *24*, 1549-1562.

84. Abdel-Hamid, M. K.; Mccluskey, A. In Silico Docking, Molecular Dynamics and Binding Energy Insights into the Bolinaquinone-Clathrin Terminal Domain Binding Site. *Molecules* **2014,** *19*, 6609-6622.

85. Ravelli, R. B.; Gigant, B.; Curmi, P. A.; Jourdain, I.; Lachkar, S.; Sobel, A.; Knossow, M. Insight into Tubulin Regulation from a Complex with Colchicine and a Stathmin-Like Domain. *Nature* **2004,** *428*, 198-202.

86. Veber, D. F.; Johnson, S. R.; Cheng, H.-Y.; Smith, B. R.; Ward, K. W.; Kopple, K. D. Molecular Properties That Influence the Oral Bioavailability of Drug Candidates. *J. Med. Chem.* **2002,** *45*, 2615-2623.

87. Goodson, L. H.; Honigberg, I. L.; Lehman, J.; Burton, W. Potential Growth Antagonists. I. Hydantoins and Disubstituted Glycines1, 2. *J. Org. Chem.* **1960,** *25*, 1920-1924.

88. Kamel Metwally, E. A., Omar Aly, Sameh El-Nabtity. Spirohydantoins Derived from 1-Tetralone: Design, Synthesis and Exploration of Their Anticonvulsant Activity and Neurotoxicity. *Bulletin of faculty of Pharmacy, Cairo University* **2007,** *45*, 149-154.

89. Rabea, S. M.; El-Koussi, N. A.; Hassan, H. Y.; Aboul-Fadl, T. Synthesis of 5-Phenyl-1-(3-Pyridyl)-1h-1, 2, 4-Triazole-3-Carboxylic Acid Derivatives of Potential Anti-Inflammatory Activity. *Arch. Pharm.* **2006,** *339*, 32-40.

90. Mosmann, T. Rapid Colorimetric Assay for Cellular Growth and Survival: Application to Proliferation and Cytotoxicity Assays. *J. Immunol. Methods* **1983,** *65*, 55-63.

91. Scudiero, D. A.; Shoemaker, R. H.; Paull, K. D.; Monks, A.; Tierney, S.; Nofziger, T. H.; Currens, M. J.; Seniff, D.; Boyd, M. R. Evaluation of a Soluble Tetrazolium/Formazan

Assay for Cell Growth and Drug Sensitivity in Culture Using Human and Other Tumor Cell Lines. *Cancer Res.* **1988,** *48*, 4827-4833.

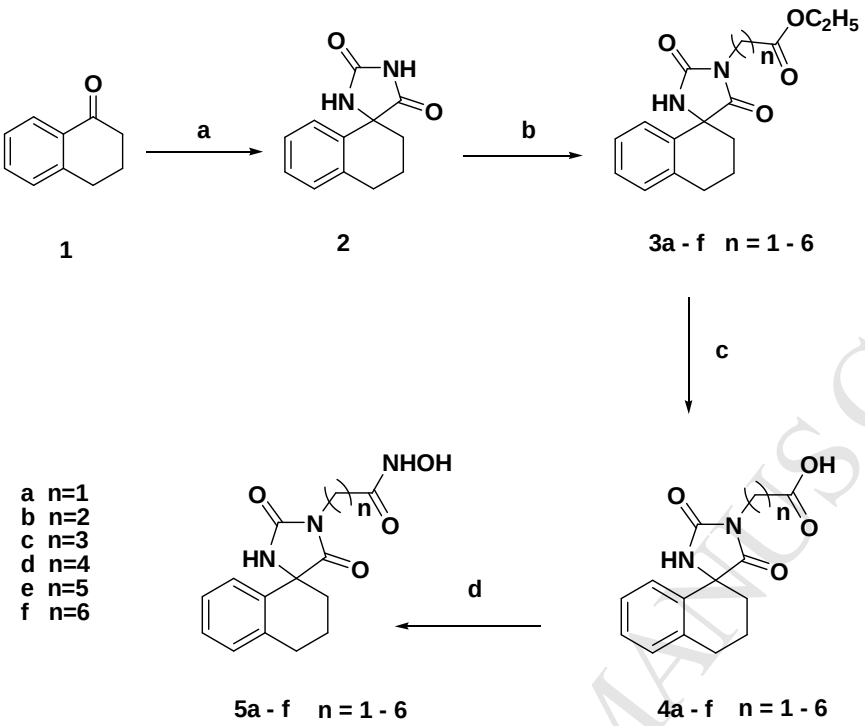


Reagents and conditions: (a) KCN, $(NH_4)_2CO_3$, 60%EtOH, 58-61°C, 48 h; (b) $Br(CH_2)nCOOC_2H_5$, $K_2CO_3$ anh. Acetone, reflux, 4 h; (c) 20%KOH, MeOH, reflux, 1 h; (d) CDI, $NH_2OH.HCl$, THF, stirr, 2 h.

**Scheme 3.** Synthesis of ε-(2,5-dioxo-3',4'-dihydro-2'H-spiro[imidazolidine-4,1'-naphthalen]-1-yl)alkanoic acids (**4a-f**) and -N-hydroxyalkanamides (**5a-f**).

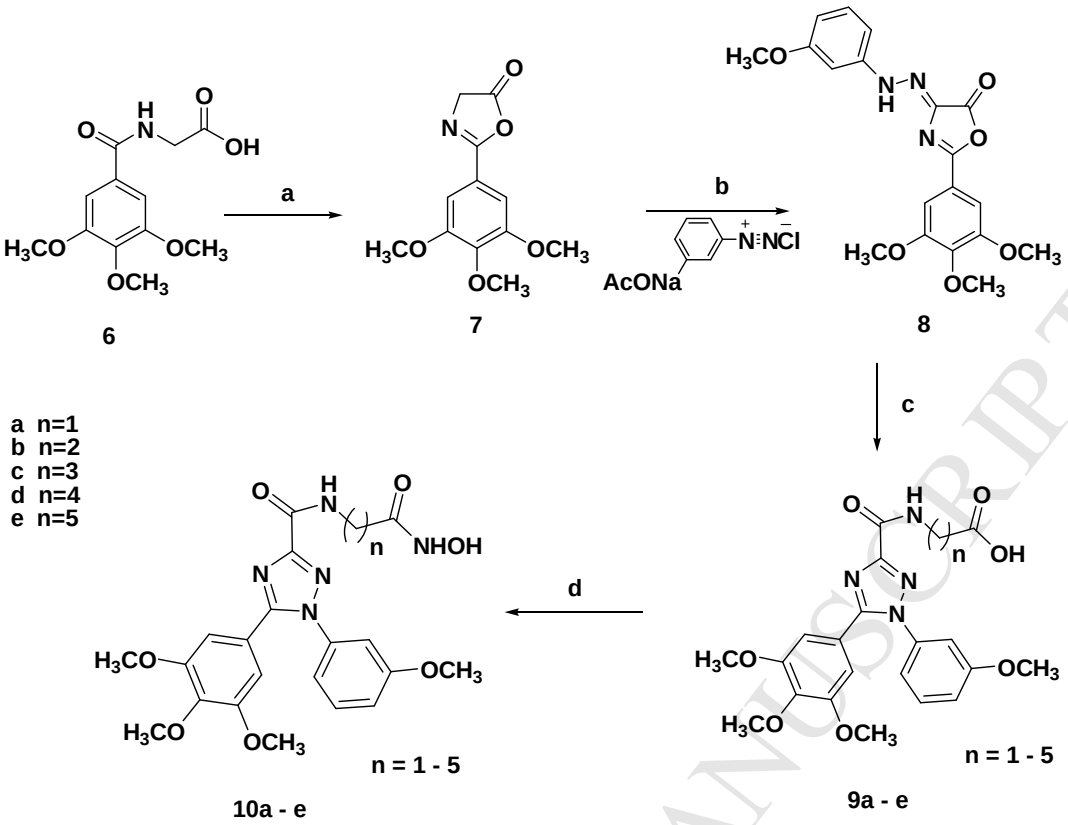


Reagents and conditions: (a) $Ac_2O$, 60°C, 2 h; (b) NaOAc; (c) $H_2N(CH_2)nCOOH$, AcOH, NaOAc, reflux, 2 h; (d) CDI, $NH_2OH.HCl$, THF, stirr, 2 h.

**Scheme 4.** Synthesis of: ε-(1-(3-methoxyphenyl)-5-(3,4,5-trimethoxyphenyl)-1H-1,2,4-triazole-3-carboxamido)alkanoic acids (**9a-e**) and -N-hydroxyalkanamides (**10a-e**).

**Table 1.** $IC_{50}$ values for anti-proliferative activity of compounds **4a-f**, **5a-f**, **9a-e**, **10a-e**, CA4, and SAHA measured using MTT assay against two cancer cell lines MCF-7, and HepG2.

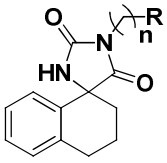

**4** and **5**

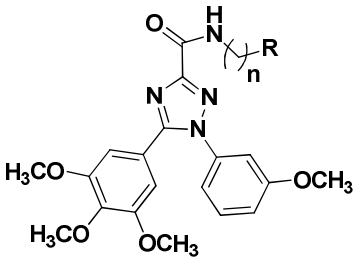

**9** and **10**

| Compound | | | $IC_{50}$ (µM)[a]/ cell line[b] | |
|---|---|---|---|---|
| **Number** | **n** | **R** | **MCF-7** | **HepG2** |
| **4a** | 1 | COOH | 1000 | 1000 |
| **4b** | 2 | COOH | 1000 | 1000 |
| **4c** | 3 | COOH | 676.08 | 1000 |
| **4d** | 4 | COOH | 1000 | 1000 |
| **4e** | 5 | COOH | 1000 | 1000 |
| **4f** | 6 | COOH | 1000 | 1000 |
| **5a** | 1 | CONHOH | 85.11 | 407.38 |
| **5b** | 2 | CONHOH | 48.98 | 162.18 |
| **5c** | 3 | CONHOH | 42.66 | 138.04 |
| **5d** | 4 | CONHOH | 19.05 | 245.47 |
| **5e** | 5 | CONHOH | 13.8 | 575.44 |
| **5f** | 6 | CONHOH | 2.56 | 169.82 |
| **9a** | 1 | COOH | 67.6 | 6.19 |
| **9b** | 2 | COOH | 1000 | 1000 |
| **9c** | 3 | COOH | 1000 | 1000 |
| **9d** | 4 | COOH | 645.65 | 1000 |
| **9e** | 5 | COOH | 245.74 | 1000 |
| **10a** | 1 | CONHOH | 14.05 | 120.23 |
| **10b** | 2 | CONHOH | 24.05 | 85.11 |
| **10c** | 3 | CONHOH | 47.56 | 48.96 |
| **10d** | 4 | CONHOH | 51.04 | 43.03 |
| **10e** | 5 | CONHOH | 57.61 | 42.07 |
| **CA4** | | | **69.6** | **0.19** |
| **SAHA** | | | **2.18** | **3.33** |

[a] The concentration (µM) that produce 50% reduction in cell growth, the number represent the average results from triplicate experiments with deviation of less than 10%.

[b] Cell lines: MCF-7, human breast adenocarcinoma; HepG2, human hepatocellular carcinoma.

**Table 1.** $IC_{50}$ values for *In vitro* HDAC inhibitory activity of **5f**, **10a**, **10e** and SAHA against HDAC1, 2, 4, and 6.

| **RESULTS** | | | | |
|---|---|---|---|---|
| | **$IC_{50}$ values (μM)**[a] | | | |
| Compound | HDAC1 | HDAC2 | HDAC4 | HDAC6 |
| **5f** | 0.027 | 0.114 | 0.0988 | 0.261 |
| **10a** | 0.058 | 0.263 | 0.198 | 0.290 |
| **10e** | 0.038 | 0.232 | 0.180 | 0.276 |
| SAHA[b] | 0.031 | 0.081 | 0.0911 | 0.0334 |

[a] Mean $IC_{50}$ value of three independent experiments, [b] SAHA: Positive reference.

**Table 1.** $IC_{50}$ values for *In vitro* tubulin polymerization inhibitory activity of **9a**, **10a**, **10e**, and CA4 using ELISA assay for β-tubulin.

| **RESULTS** | |
|---|---|
| Compound | **$IC_{50}$ values (μM)**[a] |
| **9a** | 5.87 |
| **10a** | 7.07 |
| **10e** | 4.82 |
| CA4[b] | 5.73 |

[a] Mean $IC_{50}$ value of three independent experiments,
[b] CA4: Positive reference.

**Table 1.** Types of interactions and energy scores for the complexes formed from compounds **5e**, **5f**, **10a**, **10e** and vorinostat (SAHA) with HDLP active site.

| Cpd | Types of interactions | Energy scores | |
|---|---|---|---|
| | | **CDocker energy** | **CDocker interaction energy** |
| **5e** | One hydrogen bonding with Tyr297<br>π – σ between **5e** pentamethylene chain and Phe141 | -47.03 | -55.67 |
| **5f** | One hydrogen bonding with Tyr297<br>One hydrogen bond with His132<br>π-cation bonding between **5f** aromatic ring and Lys267 | -57.26 | -51.68 |
| **10a** | One hydrogen bonding with Tyr297<br>π- π interaction between **10a** triazole ring and Phe141 | -11.63 | -57.20 |
| **10e** | One hydrogen bonding with Tyr297<br>One hydrogen bonding with Lys267 | -14.77 | -63.18 |
| SAHA | One hydrogen bonding with Tyr297<br>π- π interaction between SAHA hexamethylene chain and Phe141 | -54.62 | -54.64 |

**Table 1.** Types of interactions and energy scores for the complexes formed from compounds **9a**, **10a**, **10e**, and CA4 with the colchicine binding site of β-tubulin.

| Cpd | Types of interactions | Energy scores | |
|---|---|---|---|
| | | **CDocker energy** | **CDocker interaction energy** |
| **9a** | One hydrogen bonding between a methoxy oxygen of ring A and amino group of Gln11 in the α-tubulin subunit.<br>One hydrogen bond between the second methoxy oxygen of ring A and amino group of Lys254 in the β-tubulin subunit. | -13.18 | -54.71 |
| **10a** | One hydrogen bonding between the hydroxamic oxygen and amino group of Lys254 in the β-tubulin subunit.<br>One hydrogen bond between the terminal hydroxyl group in **10a** and carbonyl group of Asn249 in the β-tubulin subunit | -13.25 | -62.03 |
| **10e** | One hydrogen bonding between the hydroxamic nitrogen and hydroxyl group of Tyr224 in the α-tubulin subunit.<br>One hydrogen bond between the hydroxyl group and GTP | -18.41 | -71.05 |
| CA4 | Hydrogen bonding interaction between one of the methoxy oxygens of ring A and the thiol group of Cys241[1] | -13.83 | -42.33 |

1. Ravelli, R. B.; Gigant, B.; Curmi, P. A.; Jourdain, I.; Lachkar, S.; Sobel, A.; Knossow, M. Insight into Tubulin Regulation from a Complex with Colchicine and a Stathmin-Like Domain. *Nature* **2004,** *428*, 198-202.

**Table 1.** Calculated* molecular weight, log P. number of hydrogen bond acceptors and donors, molecular volume and polar surface area for compounds **5a-f** and **10a-e**.

| Compound number | Mwt | LogP | HBA | HBD | MolVol ($A^3$) | PSA ($A^2$) | Drug likeliness score |
|---|---|---|---|---|---|---|---|
| **5a** | 289.11 | 0.24 | 4 | 3 | 298.72 | 87.71 | 0.85 |
| **5b** | 303.12 | 0.54 | 4 | 3 | 315.57 | 87.69 | 0.57 |
| **5c** | 317.14 | 0.81 | 4 | 3 | 333.47 | 87.69 | 0.66 |
| **5d** | 331.15 | 1.23 | 4 | 3 | 351 | 87.69 | 0.66 |
| **5e** | 345.17 | 1.65 | 4 | 3 | 369.29 | 87.69 | 0.66 |
| **5f** | 359.18 | 2.07 | 4 | 3 | 387.19 | 87.69 | 0.66 |
| **10a** | 457.16 | 1 | 9 | 3 | 437.81 | 124.81 | 0.01 |
| **10b** | 471.18 | 1.28 | 9 | 3 | 455.76 | 124.65 | 0.11 |
| **10c** | 485.19 | 1.76 | 9 | 3 | 473.67 | 124.65 | 0.08 |
| **10d** | 499.21 | 2.24 | 9 | 3 | 491.85 | 124.65 | 0.04 |
| **10e** | 513.22 | 2.72 | 9 | 3 | 509.48 | 124.65 | 0.04 |

HBA: Hydrogen bond acceptor HBD: Hydrogen bond donor
PSA: polar surface area
*All the previous parameters are calculated using Molsoft (molecules in silico) online software.

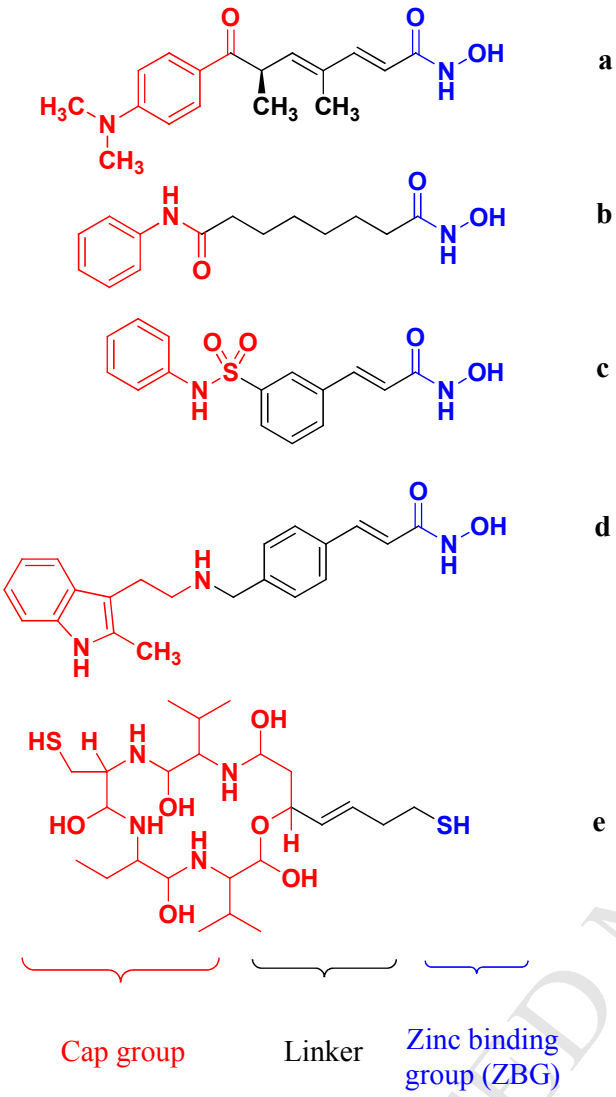


**Figure 1.** Known HDAC inhibitors; (a) Trichostatin A (TSA); (b) Vorinostat (SAHA); (c) Belinostat (PXD 101); (d) Panobinostat (LBH-589); (e) Romidepsin (FK-228).

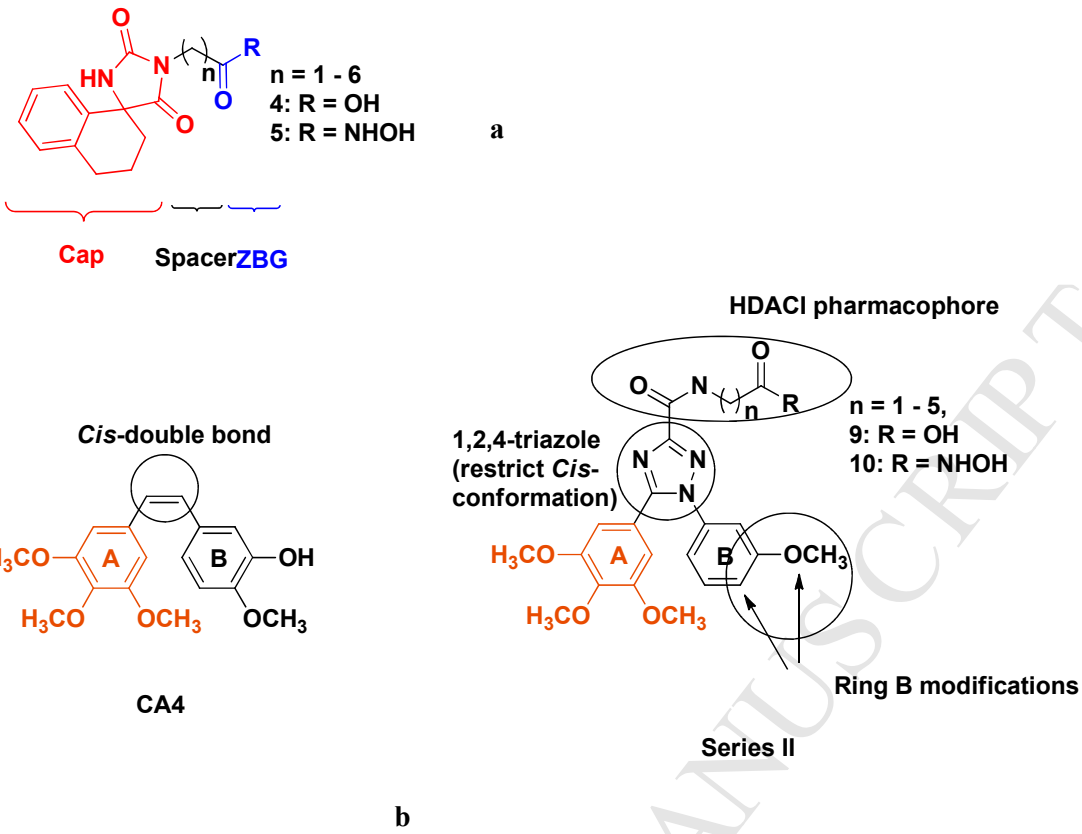


**Figure 1.** (a) General structure of 3',4'-dihydro-2'H-spiro[imidazolidine-4,1'-naphthalene]-2,5-dione derivatives; (b) General structure of 1-(3-methoxyphenyl)-5-(3,4,5-trimethoxyphenyl)-1H-1,2,4-triazole-3-carboxamide derivatives and their structural similarity with CA4.

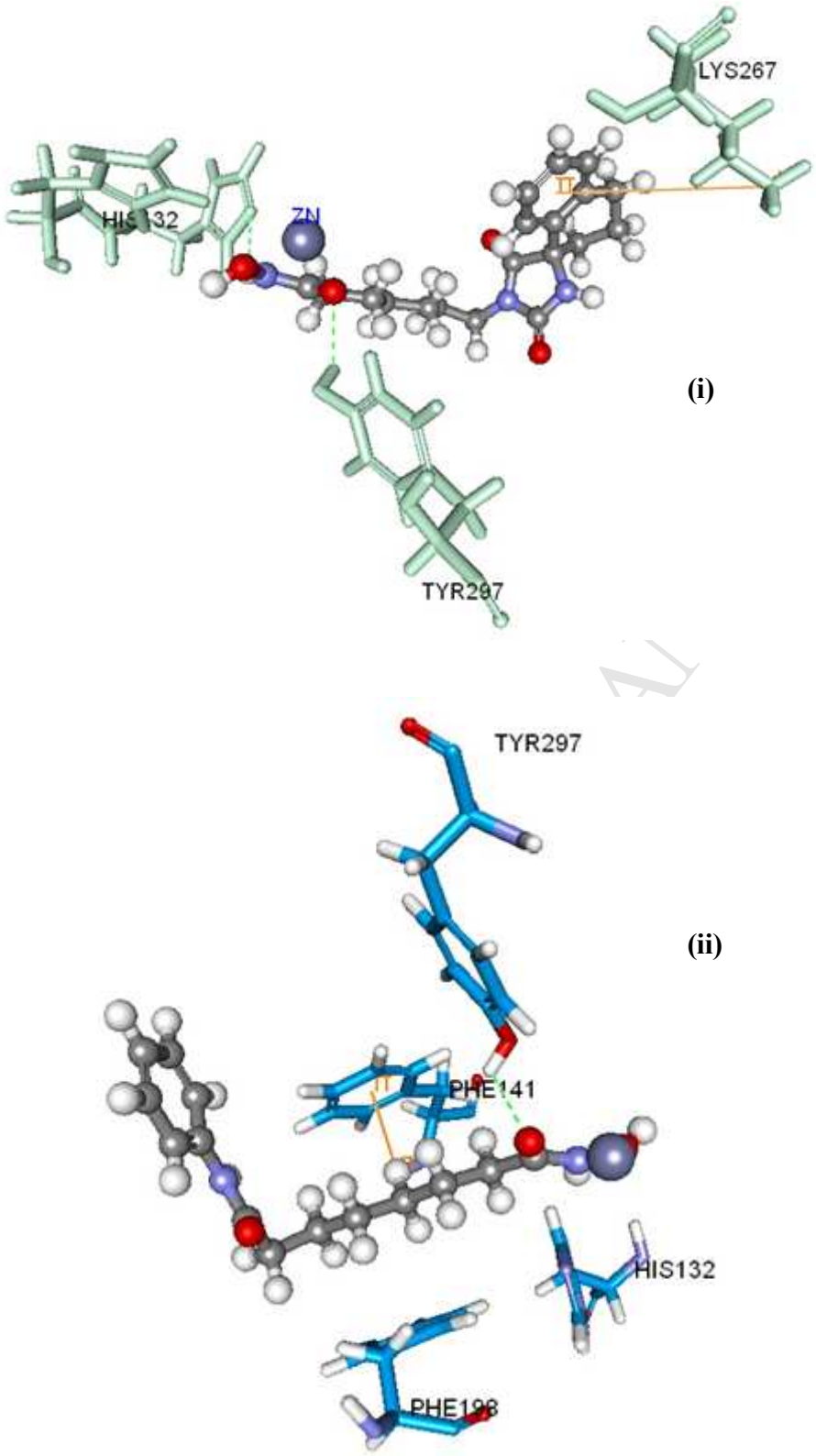


**Figure 1.** Docking of compounds (i) **5f** and (ii) vorinostat with HDLP (Histone Deacetylase-Like Protein). The residues of binding pocket are shown as stick while docked compounds are

presented as ball and stick. Dashed lines in green indicate H-bonds and yellow lines indicate π interactions.

Highlights

1. Two novel series of histone deacetylase inhibitors (HDACIs) involving two potential surface recognition moieties; 3',4'-dihydro-2'*H*-spiro[imidazolidine-4,1'-naphthalene]-2,5-dione and 1-(3-methoxyphenyl)-5-(3,4,5-trimethoxyphenyl)-1H-1,2,4-triazole-3-carboxamide were synthesized.
2. Novel compounds were evaluated for their anti-proliferative activities.
3. The mechanism was proved by evaluation of HDAC inhibitory activities.
4. Molecular Modeling studies were done to demonstrate binding modes to HDAC protein.
5. Series II have been also demonstrated as potential HDAC-tubulin dual inhibitors, promoted with structural similarities between (1-(3-methoxyphenyl)-5-(3,4,5-trimethoxyphenyl)-1H-1,2,4-triazole-3-carboxamide) nucleus, of series II, and Combretastatin A4.